studies proved that these concepts are indeed valid for certain clinical disorders of both monogenic and polygenic origins. Thus, the future looks quite promising in general. However, when the concept is applied to model a wide range of diseases, we often encounter practical limitations and obstacles for their genuine application to understand diseases, and realize their application has not been as straightforward as initially proposed. First, despite numerous published protocols, *in vitro* differentiation of iPSCs is challenging, often requiring tremendous effort for optimization until the system becomes useful in other laboratories. Second, even after differentiation is successfully achieved, a major obstacle frequently resides in limited value of the *in vitro* outcomes, which may not closely represent disease conditions.

As we have witnessed triumphal examples and experienced many practical obstacles at the same time, we are gradually recognizing ways to utilize patient iPSCs more wisely. Three years have passed since we wrote the previous review in *Laboratory Investigation*,[1] and during this time, we have had the opportunity to manage a core facility for patient iPSC research at the University of Florida. Thus, we feel this is a good time to revisit the issue of 'modeling diseases in a dish' using patient iPSCs, and try to elucidate where we are now with the technology. We target general experimental pathologists as primary readers of the present review, particularly those who are interested in starting patient iPSC research to study a disease of their interest, but not yet sure whether the direction will justify the effort. As there are many outstanding review articles available for recent technological advances in iPSCs,[3–5] here we will focus more on introducing practical issues and solutions for pathobiology applications, leaving extensive details to the references.

EXEMPLARY CASES

To understand how patient iPSC research is generally conducted, it is useful to introduce a few exemplary cases briefly, in which patient iPSCs have been wisely and beneficially utilized. As iPSCs retain genomic information from the original patient, theoretically we can analyze phenotypic and functional characteristics manifested from changes in the individual genome. Initially, early-onset monogenic disorders, where a single genetic aberration is considered to cause severe deleterious effect on cellular function, have been studied preferentially using iPSCs.

Early-Onset Monogenic Disease

An exemplary work proving the concept, 'modeling diseases in a dish' was first published in January 2009 by Ebert *et al.*[6] The authors successfully established iPSCs from patients with spinal muscular atrophy, differentiated them into motor neurons, and demonstrated the premature death of neurons *in vitro*, a phenotype reflecting the disorder. Importantly, the study further proposed that disease iPSCs could be utilized to screen novel drugs that could de-repress the *SMN2* gene, a close homolog of the mutated *SMN1* gene. SMN2 is normally not expressed in neurons but could mitigate the disease phenotype when induced. It should be noted that the *SMN2* gene only exists in humans but not in rodents, thus this type of drug screening would only be possible using human neurons.

Late-Onset Monogenic Disease

Modeling late-onset disease in a dish is a more difficult task because some environmental factors, for example, oxidative stressors, may be involved in disease progression. Nevertheless, Nguyen *et al*[7] demonstrated, for instance, that a phenotype of a familial Parkinson's disease (PD) can be evaluated *in vitro*. The authors generated iPSCs from a patient with a mutation in the leucine-rich repeat kinase 2 (*LRRK2*) gene and differentiated the iPSCs into dopaminergic neurons. The resultant dopaminergic neurons were more susceptible to oxidative stressors (hydrogen peroxide, MG-132 and 6-hydroxydopamine), compared with those from control iPSCs. The study also demonstrated that the patient iPSC-derived dopaminergic neurons had an increase in α-synuclein, which is one of the major components of Lewy bodies, a hallmark of PD pathology.

Proving the Causal Mutation and Elucidating a Novel Mechanism

LRRK2-G2019S is the most commonly identified mutation, but it is only found in a few percent of the sporadic PD patients. Genome-wide association studies suggested that many other polymorphisms in other genomic loci are linked to the disease phenotypes and clinical courses. To that end, the exact pathological mechanism caused by the *LRRK2-G2019S* mutation needed to be elucidated using isogenic controls. Reinhardt *et al*[8] applied genomic engineering technology to correct the *G2019S* mutation in patient iPSCs. They confirmed *LRRK2-G2019S* indeed induced pathological changes of dopaminergic neurons such as deficit in neurite outgrowth, defect in autophagy, increase in α-synuclein, and higher susceptibility to oxidative stress. Furthermore, the study demonstrated the *LRRK2-G2019S* mutation is associated with activation of extracellular signal-regulated kinases (ERKs), which leads to transcriptional dysregulation of CPNE8, MAP7, UHRF2, ANXA1 and CADPS2, resulting in neural degeneration. By demonstrating an ERK inhibitor-mediated amelioration of the neurodegeneration, the study indeed indicated a novel therapeutic approach for patients with PD.

Polygenic Disorder or Disease of Unknown Causes

In the case of polygenic disorders or sporadic diseases with unknown causes, it is more challenging to obtain useful outcomes using patient-derived iPSCs. Israel *et al*[9] successfully investigated neural phenotypes derived from both familial and sporadic Alzheimer's disease. One of the

	Helpful	Harmful
Internal Origin	**Strengths** ❑ Clear merits to use patient iPSCs ❑ Strong research history for the disease ❑ Accessibility to number of patients (or iPSC clones) ❑ Preexisting collaborative strengths to develop the study	**Weaknesses** ❑ May take time to establish differentiation protocols in your lab ❑ Differentiated cells may not be pure or mature enough for your study
External Origin	**Opportunities** ❑ High expectations for developing novel model systems ❑ High expectations from societies of particular diseases ❑ External and internal grant opportunities	**Threats** ❑ Competitors working on similar directions ❑ Competing animal models

Figure 1 SWOT analysis before start patient iPSC research. It is critical to analyze all the strengths and potential problems you have before you initiate patient iPSC research. A local iPSC core facility may also assist you to analyze individual projects and create a research design.

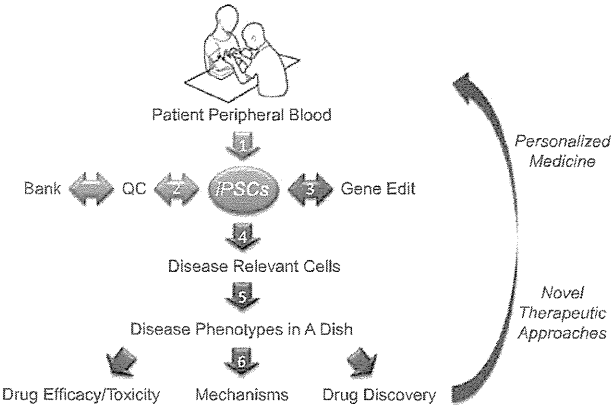

Figure 2 A typical work flow of patient iPSC research and tips for individual steps. (**1**) iPSC generation (~3 weeks)—multiple clones from multiple patients using non-integrating reprogramming vectors; (**2**) Quality control (QC) and storage (1–4 weeks)—first by morphology and pluripotency markers, then ideally by gene expression profiling, teratoma formation, karyotyping, exome analysis, and mycoplasma testing; (**3**) Isogenic controls made by gene editing serve as ideal controls; (**4**) Differentiation (2–10 weeks)—consult a local iPSC core or colleagues to identify the best available protocols; (**5**) Disease recapitulation—set realistic goals to demonstrate unique pathological changes *in vitro*; (**6**) Study further disease mechanisms—molecular 'omic' analyses are often used here. 'Green' highlighted parts are usually taken care by a local iPSC core facility (if desired), whereas 'blue' highlighted parts will typically be performed by individual investigators.

two sporadic patient's iPSCs showed higher levels of the pathological markers amyloid-β (1-40), phosphor-tau(Thr231) and active glycogen synthase kinase-3β (aGSK-3β), as those derived from familial Alzheimer's disease, while the other case did not. These observations offered new opportunities to investigate the mechanisms underlying heterogeneity among sporadic cases. For such studies, however, a larger number of patients and controls would ideally be required.

Imprinting Disorders

In addition to genetic diseases, the iPSC models facilitate investigation of epigenetic-related diseases such as Beckwith–Wiedemann syndrome, Silver–Russell syndrome, Angelman syndrome and Prader–Willi syndrome. Unlike genetics based on the DNA sequence, epigenetic processes involve DNA methylation and histone modulation. One of the most important epigenetic phenomena is genomic imprinting by which genes are expressed in a parent-of-origin-specific manner. Abnormality of the imprinting mechanism during development causes epigenetic diseases. The methylation status of imprinting genes is maintained during iPSC generation and subsequent cultivation, implying that imprinting disease iPSCs are worth investigating to elucidate mechanism of imprinting abnormality.[10] Patient iPSCs from Angelman and Prader–Willi syndrome have been established and utilized for examination of epigenetic and transcriptomic abnormalities, and for testing compounds aimed at correcting the epigenetic aberrations.[11,12] One must use caution when analyzing epigenetic aberrations in imprinting disease iPSCs because the process of iPSC generation is associated with epigenetic dynamics that may bias interpretation.[13] However, iPSCs with *in vitro* multipotency have been an invaluable tool to clarify molecular mechanisms as a simulator of developmental defects.[14,15]

PRACTICAL ADVICE BEFORE YOU BEGIN

These exemplary cases certainly make us feel hopeful that we can apply patient iPSCs to various diseases. Taking all the progress and current issues into consideration, which we discuss more in detail in the following section, we have compiled practical tips you may find useful when starting patient iPSC research. First, it is essential to analyze whether the project is worth pursuing, as with any other new research projects. A SWOT analysis, for an example as shown in Figure 1, will guide you to identify the potential internal and external strengths and weaknesses of your direction. Unfortunately, the field is highly competitive, and the funding is scarce; thus it is critical to fully analyze the status of your project before beginning. In the end, the most important factor in the analysis is whether you have unique and significant question(s) that are likely answered using patient iPSCs.

When the analysis is positive, Figure 2 illustrates an actual workflow of the study with estimated time lines. Unless you have extensive experience in human pluripotent stem cell culture, it is easiest to consult with an iPSC core facility or colleagues to generate patient iPSCs. In a typical study of a monogenic disorder, generation of three iPSC clones from three individual patients is minimally required, along with an equivalent number of controls; however, such number can vary considerably depending on your questions. The quality of iPSC clones should also be controlled by the core facility to

Table 1 List of iPSC banks and registries by disease

Diseases	Institute	Website
General	Corriel Institute/NIGMS	http://ccr.coriell.org/Sections/Collections/NIGMS/ipsc_list.aspx?PgId=696
	American Type Cell Collection	http://www.atcc.org/Products/Cells_and_Microorganisms/Stem_Cells/Human_IPS_Pluripotent.aspx
	RIKEN Bioresource Center Cell Bank	http://www.brc.riken.jp/lab/cell/english/index_hps.shtml
	Wi-Cell	http://www.wicell.org/home/stem-cell-lines/order-stem-cell-lines/obtain-stem-cell-lines.cmsx
	Boston University, Center for Regenerative Medicine	http://www.bu.edu/dbin/stemcells/ips_cell_bank.php
	U MASS International Stem Cell Registry	http://www.umassmed.edu/iscr/Genetic-Disorders-Lines/
	U Connecticut Stem Cell Core	http://stemcellcore.uchc.edu/services/distribution.html
	Harvard Stem Cell Institute	http://stemcelldistribution.harvard.edu/shoppingCart/index
Neural	Corriel Institute/NINDS	http://ccr.coriell.org/Sections/Collections/NINDS/ipsc_list.aspx?PgId=711&coll=ND
Mental	NIMH Stem Cell Center	http://nimhstemcells.org/catalog.html

Currently available information of iPSC bank and registry (June 2014). Please note that the list here may not cover all the available sites.

meet the current standard, as discussed later. If patient iPSC clones or fibroblasts already exist in publicly available libraries, you can save substantial amount of time and cost. Table 1 shows a list of disease iPSC bank and registry, in which you may be able to find the lines of your interest. Additional information is available in a recent review article specifically discussing this topic.[16]

As we discuss later, iPSC differentiation should ideally be performed in collaboration between your lab and the iPSC core or a person who has iPSC expertise. In the steps of disease recapitulation and further mechanism studies, it is particularly important to set practical goals for patient iPSC research. First, you should accurately estimate purity, quantity and maturation status of the resultant iPSC-derived differentiated cells. Depending on those factors, you can identify what types of assays can be performed with the prepared cells. In general, patient iPSCs will hold the most value in identifying molecular changes caused by pathogenic mutations in certain human cell types. 'Omic' level screening will be particularly useful there; and isogenic iPSC clones with the mutation corrected through gene editing would serve as ideal controls in such tests, as discussed later.

TECHNICAL IMPROVEMENT AND REMAINING CHALLENGES

iPSC Generation

Viral methods

Methods for achieving reprogramming have progressed significantly from the groundbreaking work completed by Yamanaka and colleagues. The variety of reprogramming approaches stems from an interest to develop methods that do not integrate DNA into the host genome, making them feasible for eventual use in clinical applications. Virus-mediated reprogramming is commonly used for its capacity to efficiently transduce cells of interest. Original methods using retrovirus[2,17] and lentivirus[18] remain widely used. The disadvantage is that these viruses integrate transgenes randomly into the host genome upon infection. This has the potential to cause unpredictable changes in the genome and result in aberrant transgene expression, which can potentially impact data interpretation and differentiation potential. Although scientists have devised ways to remove the transgenes after reprogramming is complete (using loxP sites and Cre recombinase),[19] it is still necessary to thoroughly screen clones for confirmation of excision and loxP site retention that may alter endogenous gene expression. For these reasons, methods to reprogram cells have since focused on naturally non-integrating approaches.

Improvements using viruses that do not integrate into the genome, including adenovirus and Sendai virus, are becoming increasingly popular. The use of adenovirus was first applied to iPSC reprogramming shortly after the initial reprogramming reports.[20,21] Adenovirus was chosen for its inability to integrate into the genome and ability to provide high transgene expression for a limited amount of time as the virus is reduced with each cell division. Although successful, the incidence of tetraploid cells following reprogramming has limited its usefulness.[20]

Sendai virus has recently been developed for reprogramming because it is non-cytopathic and remains in the cytoplasm of host cells.[22] In addition, it has the ability to reprogram peripheral blood mononuclear cells (PBMCs) in addition to other somatic cells (including fibroblasts). In addition to the non-integrating nature of this virus, it is cleared by culturing cells at an elevated temperature, or treatment with siRNA against the large protein (L-gene) of

the virus. Recently, a modification has also been introduced that enables clearance by microRNA 302L, naturally produced by pluripotent cells, which recognizes an inserted microRNA targeting sequence that was incorporated into the vector (Nakanishi, personal communication).

Non-viral methods

Non-viral methods include minicircle and episomal plasmids, piggyBac transposon, RNA transfection, protein transduction, and microRNA transfection. Traditional transfection was successfully used to reprogram mouse cells using polycistronic plasmids.[23,24] However, extensive screening was necessary to find clones without integration. In addition, repeated transfections were necessary to maintain high transgene expression. Minicircle DNA was first applied to reprogram adipose stem cells.[25] Polycistronic minicircle is advantageous because transfection efficiency is improved and it is diluted out more slowly during cell division, thus reducing the number of transfections required. Unfortunately, both conventional and minicircle DNA reprogram at much lower efficiency and also require more hands on time due to multiple transfections. Episomal plasmids can be stably introduced into cells using drug selection, and can be removed after drug selection is discontinued. Yu *et al*[26] first showed feasibility of this method in 2009 by reprogramming human foreskin fibroblasts, although unfortunately this method also yielded low efficiency. The piggyBac transposon system enables the removal of all exogenous elements, cleaner than the Cre-loxP system. In 2009, multiple groups demonstrated high efficiency reprogramming using tetracycline-inducible or polycistronic expression of the reprogramming factors.[27–29] Although removal of the transgenes was demonstrated by sequencing, transposase-mediated excision of transgenes was shown to also induce microdeletion of genomic DNA, which could pose a problem for future use.

Methods described thus far carry the risk of unexpected persistence or genetic modification. To circumvent this, scientists have been devising methods, which do not introduce DNA into the host cell. mRNA synthesized *in vitro* from cDNA of the reprogramming factors was demonstrated to be successful in 2010.[30] This method utilized host cells translation machinery, although it requires five consecutive transfections to be successful. Protein delivery is an alternative to nucleic acid introduction. Harnessing the ability of reprogramming factors tagged with C-terminus poly-arginine domains to transduce through the cell membrane, two groups showed feasibility.[31,32] Protein delivery method eliminates the need to screen for integration of transgenes. However, efficiency was lower, and multiple rounds of transduction were necessary. In 2011, mature double-stranded microRNA including mir-200c, mir-302s and mir369s family of microRNAs were shown to reprogram somatic cells by direct transfection.[33] Although this method resulted in lower efficiency, it provides a viable method compatible with clinical use.

Ultimately, these methods and modifications have laid the groundwork for improving methodology. Combination of these methods with small molecules has been shown to improve reprogramming. In 2013, Deng's group used a cocktail of seven compounds to reprogram mouse somatic cells into iPSCs at efficiency comparable to standard reprogramming techniques.[34] The ability to apply this technique to human cells would be an exciting advance in the field. Although many methods focus on efficiency, it is important to note that efficiency alone is not the most important aspect of the reprogramming process. In the end, it is more important to obtain a number of high quality iPSCs clones. Generally, fewer than 10 clones per individual are needed, especially if using a non-integrating method where exhaustive transgene screening is not necessary.

Practical considerations

Starting cell type before reprogramming is an important consideration. Dermal fibroblasts and PBMCs are the most common starting cells, and while most methods nearly always reprogram dermal fibroblasts successfully, using a method that also works for PBMCs increases flexibility. Benefits include reduced processing time (biopsy outgrowth can require up to 1 month *vs* isolation of PBMCs from a blood draw can be completed within an hour). In addition, a blood draw is less invasive and particularly useful for obtaining cells from pediatric patients. Ultimately, starting cell type may vary depending on the questions to be asked. If initial assays using fibroblasts can be useful for disease understanding, it may be advantageous to reprogram those cells. Regardless of delivery method (virus, plasmid and so on), utilizing polycistronic plasmids to introduce all reprogramming factors at once is easier and increases the likelihood of successfully reprogramming.

Commercial availability of multiple reprogramming methods is also increasing. Although cost may be an issue, it is possible to send samples to be reprogrammed using various non-integrating methods or to purchase ready to use reagents to complete the procedure in the lab. In addition, it is important to realize the reprogramming process itself is not the only barrier to overcome. It is imperative to learn proper culture techniques. To this end, many commercially available cell culture media are available (Life Technologies, ReproCell, Stem Cell Technologies and so on) that can ease the transition for researchers who are new to the culture techniques required to propagate these cells. Even for seasoned scientists, commercial protocols and products enable quick improvements and it is advantageous to keep up to date to reduce labor and improve quality of iPSC culture.

In addition to various culture media, there are also a number of different substrate iPSCs can be cultured on (mouse embryonic fibroblasts, Matrigel, Vitronectin, Geltrex and so on). In addition, iPSCs themselves are generally an

intermediate resource before differentiation to various lineages. As such, the vast variety of differentiation protocols generally has different starting cell culture conditions. Usually, these are referred to as feeder dependent or feeder free. For this reason, it may be advantageous to generate frozen stocks cultured by feeder-dependent and feeder-free techniques to reduce the labor involved if testing out a number of protocols.

Quality Control

Variability within iPSC clones (either genetic, epigenetic or phenotypic) has been a concern in patient iPSC research. Unless each iPSC clone is carefully evaluated, researchers could potentially run into issues with data misinterpretation when using this approach.

Quest for genome stability

To investigate characteristics of iPSCs derived from monogenic disorders, one of the important issues is to validate retention of the gene mutation in iPSCs and to identify additional mutations introduced during iPSC generation. By comparing genomes of parental cells and iPSCs, exome analysis may be a prerequisite for subsequent medical research of pathogenesis and drug discovery. Whole-exome analysis covering protein-coding sequences is sufficient to investigate pre-existing and additional mutations, although the recent platform of exome analysis has expanded to include not only coding but also untranslated, non-coding RNA and their adjacent regions. The number of single-nucleotide mutations per cell genome was estimated from 22 human iPSCs by extensive exome analysis on protein-coding sequences.[35] Generally, iPSCs are considered to have a comparable nucleotide substitution rate independent of donor cells, except for cells from patients with a genome instability syndrome, a DNA repair disorder or a DNA damage response syndrome. However, acquisition of novel mutations during passages is indeed unavoidable, and banking of early passage iPSC clones is therefore essential once suitable disease iPSCs are established and characterized.

Quest for quality control

In addition to genomic analysis, general characteristics of disease iPSCs such as morphological analysis, *in vitro* differentiation by embryoid body formation, teratoma formation by injection of iPSCs into immunodeficient animals, karyotypic analysis, short tandem repeat analysis, pluripotency markers such as Oct4/3, Sox2, Nanog, SSEA4, Tra-1-60 and Tra-1-81, and gene expression of exogenous and endogenous pluripotency-associated genes are usually performed. Before banking, contamination of mycoplasma, bacteria, virus and endotoxins should ideally be tested. Generally, morphology of iPSCs provides us enormous information including purity, quality, transformation, undifferentiated state and other cell contamination. In addition to these standard quality controls, profiling of RNA expression, DNA methylation and glycans can be added for monitoring when necessary.[10,13,36,37] These comprehensive analyses would also elucidate pathogenic states such as aberrant genomic methylation and gene expression of patient iPSCs.

Quest for suitable controls of disease iPSCs

In addition to disease-derived iPSCs, preparation of suitable control iPSCs are required for elucidation of disease mechanisms and drug discovery. One of the ideal controls is genetically corrected iPSCs. To correct gene mutation in disease iPSCs, ZFN, TALEN and CRISPR/Cas-based methods for genome editing can be used. Alternatively, introduction of exogenous genes that are mutated in disease iPSCs may be used, but the expression level of the exogenous gene may bias phenotypes. Another control is iPSCs obtained from the same age, gender and ethnic group. Usually, iPSCs from more than three independent patients and from more than three independent healthy donors need to be analyzed to conclude that observed pathogenic phenotypes are due to endogenous genotypes of the disease iPSCs. However, genetic correction and preparation of age-, gender- and ethnic-matched controls is labor intensive. To circumvent this, commonly available iPSCs from healthy donors may be used for comparison. MRC5-derived (fetal lung fibroblast) iPSCs have been utilized as a control in several previous reports,[13,37–41] and can be obtained from the public bank. If MRC5-iPSCs do not demonstrate pathogenic phenotypes that disease iPSCs do under the same experimental condition, MRC5-iPSCs would serve as a practical control.

Differentiation

Lack of practical differentiation protocols

Depending on the desired disease or field of study, there may be ample protocols for investigators to turn to (as in the case of neurodegenerative disease modeling).[3,5] However, unless the particular lab is well versed in the biology of both pluripotent stem cells and differentiated cell types, the likelihood of reproducing a protocol in a reasonable time is uncertain. In general, differentiation protocols take advantage of particular cytokines, culture media and extracellular matrices, thus making these protocols quite expensive. Often, after differentiation, cell populations of interest need to be separated using specific surface markers to achieve sufficient purity. In addition to the expense, most protocols are time consuming and slow in data collection. In general, common obstacles in published differentiation protocols include low reproducibility, low yield, high cost and multiple steps, which often utilize complicated procedures. Thus, except for a few relatively straightforward lineages such as neural progenitors, we are still lacking very practical protocols to prepare a large number of disease-relevant cell types. Developing simple, easy and affordable methods, where the process can be applied to robust

large-scale cell differentiation from patient iPSCs, is truly desired in the field.

Uncertain quality of differentiated cells

Depending on the cell type, iPSC differentiated cells may not proliferate well in the long term. As with human primary cells, doubling times while maintaining proper phenotype will most likely be limited, making it more difficult to carry out desired experiments. Furthermore, the possibility of freezing a batch of cells for later use may be unrealistic, giving investigators a 'one shot' per differentiation scenario to obtain meaningful data. This can become taxing if a differentiation protocol takes months from start to finish as in the case of vascular cell differentiation with a 2-month long protocol.[42] Also, unless the differentiation protocol is well established in an investigator's own hands, a portion of the obtained cells will need to be used to assess the proper phenotype. Despite a successful differentiation protocol, investigators may run into issues if these cells are to be used in functional assays. iPSC-derived cells may have the proper phenotype but may be too immature to also possess the normal function of the cells. In that case, investigators will have to optimize such conditions for their specific interests keeping in mind the physiological relevance of their *in vitro* assays.

Practical considerations

Although there remain many issues to be improved, some iPSC differentiation protocols are relatively straightforward, and have been successfully used by multiple groups to obtain mesoderm,[42–44] endoderm[45] and ectodermal[46–48] lineages. These protocols utilize available materials, the procedures are uncomplicated, the methods include simple cell purification steps such as sorting, and their reproducibility and usefulness have been demonstrated by other investigators. There are many additional protocols available in the literatures (many that share commonalities, while others are distinct). As the field is constantly changing, updated information is best obtained through an iPSC core facility or colleague scientists. We emphasize here again that one should try to reproduce the protocol(s) in a side-by-side collaboration with a scientist who has expertise in iPSCs and another scientist with experience of the targeted differentiating lineage. Knowing the biology of both ends, the cells you start with and those you end up with, is critical to reproducing protocols in a reasonable time.

Disease Modeling

How to fill the discrepancies from real disease

Although generation of disease-relevant cell types from patient-derived iPSC is a standard strategy for studying a 'disease in a dish' as described above, many human diseases arise from multicellular interactions in the context of tissue architecture, organ or whole-body homeostasis. Therefore, it is essential to further advance model systems to represent a more complex physiological environment similar to the body. When your hypothesis requires the interactions of different cell types for pathogenesis, multiple cell types in a co-culture setting will certainly provide further functional insights for the disease. As an exemplary work, the co-culture of glial cells from ALS iPSCs with neurons from normal iPSCs demonstrated the non-cell autonomous effect of diseased glial cells for aberrant survival of neurons.[49] Similarly, aberrant controls in vasculature tone would be better understood when co-culturing endothelial and vascular smooth muscle cells together rather than using a single cell type.

Admirably, iPSCs possess pluripotency comparable to embryonic stem cells (ESCs), which are originated from the embryonic blastocyst stage embryo. Both iPSCs and ESCs are competent to early developmental cues. Once proper cues are given, initial specification occurs to induce differentiation. The multiple types of differentiated cells are autonomously organized and interact with each other leading to subsequent fate specification like the cascade of embryonic development. To take maximum advantage of this self-organizing ability of pluripotent stem cells, several groups have developed sophisticated 3D culture protocols for making organoid structures *in vitro*. One example is the so-called 'mini-brain' consisting of tissue layers that mimic the brain cortex. Using this culture technique, Knoblich's group demonstrated that iPSCs derived from a microcephalic patient indeed formed a smaller brain than iPSCs from a healthy control.[50] Similarly, several organoid culture techniques for iPSCs have evolved to generate other tissue types and organs (optic cup, pituitary gland).[51,52] Lack of vascular supply is the major limiting factor to grow more functional units in organoid culture. Remarkably, Taniguchi's group was able to generate a transplantable small liver unit from human iPSCs. They co-cultured hepatic endoderm cells differentiated from iPSC with human mesenchymal stem cells and human umbilical vein endothelial cells in a loosely solidified extracellular matrix. These cells autonomously formed the functional units of the liver *in vitro* with the support of microvasculature. Upon transplantation of the unit into immunodeficient mice, the liver bud quickly connected to the host vascular networks and further functional maturation occurred.[53]

Advances in differentiation protocols heavily rely on our knowledge of the molecular mechanisms of embryonic development. Our knowledge is not sufficient to provide the optimal environment for desired morphogenesis from iPSC *in vitro* culture. Nevertheless, simple inoculation of iPSCs into immunodeficient animals is able to form teratomas, which comprise cells from all three germ layers (endoderm, mesoderm and ectoderm). As mature tissue organization (gut epithelial, cartridge and so on) can be observed in the tumor, it will be feasible to assess the histopathological phenotype of patient-derived iPSC using this methodology. For instance, iPSCs from dominant genetic disorders with oncogenesis may develop cancer in teratomas over time. Patients with familial adenomatous polyposis develop

adenoma and adenocarcinoma in colon. Similarly, iPSCs from familial adenomatous polyposis may generate adenoma and adenocarcinoma in colon-like mucosa in teratomas. iPSCs from degenerative disorders may exhibit degeneration or apoptosis of cells in corresponding tissues of teratomas. It is also noteworthy that histopathological analysis of implanted cells into immunodeficient animals may support *in vitro* phenotypes of iPSCs during the differentiation process.

To model systemic disease, it is compelling to reconstitute the human pathological process in experimental animals. For example, type I diabetes is recognized as a type of autoimmune disease, in which three major cell lineages (hematopoietic cells, pancreatic β cells and thymus epithelial cells) have important roles. Melton's group has reconstituted the human version of these three lineages into animals by transplantation into immunodeficient mice.[54] A more rigorous approach is led by Nakauchi's group, where they successfully generated a whole kidney or pancreas derived from iPSCs in the pig by blastocyst complementation. They transferred donor pig iPSC into pancreatogenesis- or nephrogenesis-disabled blastocyst stage pig embryos, and demonstrated the embryos were born as chimeras having pancreas or kidney exclusively derived from the donor pig iPSCs.[55] Any blastocyst complementation using human iPSC into animals has not been performed yet because of ethical issues, but theoretically it is feasible to generate whole functional human organs in animals using the same strategy. This humanized animal or hybrid animal approach using patient-derived iPSC would be a next-generation disease model for studying human pathology.

Gene Editing

Rapidly evolving gene-editing technology has been shown valuable in patient iPSC research as well, as described above with an exemplary case.

TALEN

Transcription activator-like effector nucleases (TALENs) are composed of a DNA-binding domain that is capable of directing the *Fok*I nuclease to a specific target site. Two TALENs, recognizing left and right arms of the target site, respectively, can bring two *Fok*I monomers close together for the formation of a functional dimer, which generates a DNA double-strand break (DSB) on the target site.[56,57] The TALEN-induced DSBs activate the DNA repair system within cells, which stimulates non-homologous end joining (NHEJ) in the absence of a homologous DNA template. The error-prone nature of this repair mechanism results in the introduction of nucleotide mismatches, insertions or deletions. However, in the presence of a homologous template DNA, the DSB triggers homologous recombination, introducing desired DNA sequence alterations. The TALENs have rapidly gained prominence as a novel genome-editing tool, which were successfully applied to create site-specific gene modifications in model organisms such as yeast, plants, zebra fish, mouse, rat and human cells, including human pluripotent cells.[58–62] TALEN has also been used to generate single base-pair mutations, linking single-nucleotide polymorphisms to specific human disease.[63] Furthermore, TALENs have even been utilized to eliminate the mutant form of mitochondrial DNA from patient-derived cells.[64] Currently, TALEN plasmids targeting 18 740 protein-coding human genes have been assembled using a high-throughput Golden-Gate cloning system.[65] Delivery of these TALENs can be achieved by injection of DNA or mRNA encoding TALENs or even the TALEN proteins directly.[62,66,67]

CRISPR

The CRISPR system is another effective genome-editing tool, which utilizes Cas9 nuclease to cleave DNA and chimeric guide RNA (gRNA) to target Cas9 to a specific region in the genome.[68,69] The Cas9-gRNA-mediated genome editing has been shown to have improved efficiencies over TALENs and it is also easier to implement.[68–72] Moreover, it allows simultaneous editing of more than one site through expression of multiple gRNAs.[68,69] This approach was used to create mice carrying five different mutant genes in a single step,[73] and also was shown to generate large deletions of genomic regions by directing Cas9 cleavages at the two sites flanking the desired deletion.[68] Wu *et al*[74] have even shown in mice that a dominant mutation in *Crygc* gene that causes cataracts could be rescued by a Cas9-mediated DSB on the mutant allele, which triggered homology-directed repair based on the endogenous WT allele. More recently, a clone library encoding short gRNAs targeting all open reading frames in the human genome has been generated. Combined use of this library with Cas9 enabled the generation of random gene knockouts in the human genome, which can be screened for desired phenotypes to link genes to their functions.[75,76] The CRISPR technology has been used to cure a mouse model of a human fatal liver disorder (type I tyrosinemia) caused by a single genetic mutation in the fumarylacetoacetate hydrolase gene.[77] This defect in tyrosine catabolism causes toxic accumulation of the amino acid, leading to liver failure. CRISPR-mediated genome editing could one day help treat many diseases caused by single mutations, such as hemophilia and Huntington's disease.

A mutant version of the Cas9 was further reported which cleaves only one strand of the target DNA, generating single-strand nicking, thus favors HR DNA repair over NHEJ (error prone), increasing desired DNA changes over random mutations.[70] Recently, a nuclease-defective Cas9 enzyme has been utilized to label genomic loci, allowing for visualization of *in vivo* of their partitioning in live cells.[78] Most interestingly, the catalytically inactive Cas9 nuclease, in complex with a gRNA, can bind to a specific site, which physically blocks the RNA polymerase, thus silencing the target gene.[79] Similarly, the catalytically inactive Cas9 was fused to known transcriptional activator domains and targeted to specific promoter regions by corresponding gRNAs, upregulating the target gene expression.[80] The

ability to artificially control the expression of specific target genes not only enables us to better understand gene functions but also to manipulate cell fate through controlled expression of desired sets of pathway genes.

CONCLUDING REMARKS

Undoubtedly, patient iPSCs are an enduring asset for experimental pathology studies, with some exemplary applications introduced above and many more in published literature. Additional technical improvement, particularly in iPSC differentiation methods and three dimensional cultures, as well as expansion of patient iPSC banking, will further accelerate the field. From a pathologist perspective, patient iPSC banking will serve as a powerful addendum to existing tissue banks. Their value is unlimited, as once established, they serve as an enduring and expandable resource for live patient cells. For instance, it is almost impossible to obtain hepatocytes from a rare metabolic disease through liver biopsy of a large number of patients at one given time and place. However, through iPSC banking, such resources will be available to any researcher, any place in the world, and at any time. Banking iPSCs of large patient cohorts with a clinical and GWAS database would be particularly useful in order to identify molecular mechanisms underlying certain genetic links to the disease or individual patients' drug efficacy and toxicity. The future rests on how properly we prepare the resource and how wisely we use it.

ACKNOWLEDGMENTS

We thank Ms Erika Suzuki for her secretarial work.

DISCLOSURE/CONFLICT OF INTEREST

The authors declare no conflict of interest.

1. Hankowski KE, Hamazaki T, Umezawa A, *et al.* Induced pluripotent stem cells as a next-generation biomedical interface. Lab Invest 2011;91:972–977.
2. Takahashi K, Yamanaka S. Induction of pluripotent stem cells from mouse embryonic and adult fibroblast cultures by defined factors. Cell 2006;126:663–676.
3. Sandoe J, Eggan K. Opportunities and challenges of pluripotent stem cell neurodegenerative disease models. Nat Neurosci 2013;16:780–789.
4. Cherry AB, Daley GQ. Reprogrammed cells for disease modeling and regenerative medicine. Annu Rev Med 2013;64:277–290.
5. Tabar V, Studer L. Pluripotent stem cells in regenerative medicine: challenges and recent progress. Nat Rev Genet 2014;15:82–92.
6. Ebert AD, Yu J, Rose Jr. FF, *et al.* Induced pluripotent stem cells from a spinal muscular atrophy patient. Nature 2009;457:277–280.
7. Nguyen HN, Byers B, Cord B, *et al.* LRRK2 mutant iPSC-derived DA neurons demonstrate increased susceptibility to oxidative stress. Cell Stem Cell 2011;8:267–280.
8. Reinhardt P, Schmid B, Burbulla LF, *et al.* Genetic correction of a LRRK2 mutation in human iPSCs links parkinsonian neurodegeneration to ERK-dependent changes in gene expression. Cell Stem Cell 2013;12:354–367.
9. Israel MA, Yuan SH, Bardy C, *et al.* Probing sporadic and familial Alzheimer's disease using induced pluripotent stem cells. Nature 2012;482:216–220.
10. Hiura H, Toyoda M, Okae H, *et al.* Stability of genomic imprinting in human induced pluripotent stem cells. BMC Genet 2013;14:32.
11. Yang J, Cai J, Zhang Y, *et al.* Induced pluripotent stem cells can be used to model the genomic imprinting disorder Prader-Willi syndrome. J Biol Chem 2010;285:40303–40311.
12. Chamberlain SJ, Chen PF, Ng KY, *et al.* Induced pluripotent stem cell models of the genomic imprinting disorders Angelman and Prader-Willi syndromes. Proc Natl Acad Sci USA 2010;107:17668–17673.
13. Nishino K, Toyoda M, Yamazaki-Inoue M, *et al.* DNA methylation dynamics in human induced pluripotent stem cells over time. PLoS Genet 2011;7:e1002085.
14. Cruvinel E, Budinetz T, Germain N, *et al.* Reactivation of maternal SNORD116 cluster via SETDB1 knockdown in Prader-Willi syndrome iPSCs. Hum Mol Genet 2014 (e-pub ahead of print).
15. Martins-Taylor K, Hsiao JS, Chen PF, *et al.* Imprinted expression of UBE3A in non-neuronal cells from a Prader-Willi syndrome patient with an atypical deletion. Hum Mol Genet 2014;23:2364–2373.
16. McKernan R, Watt FM. What is the point of large-scale collections of human induced pluripotent stem cells? Nat Biotechnol 2013;31: 875–877.
17. Takahashi K, Tanabe K, Ohnuki M, *et al.* Induction of pluripotent stem cells from adult human fibroblasts by defined factors. Cell 2007; 131:861–872.
18. Yu J, Vodyanik MA, Smuga-Otto K, *et al.* Induced pluripotent stem cell lines derived from human somatic cells. Science 2007;318:1917–1920.
19. Soldner F, Hockemeyer D, Beard C, *et al.* Parkinson's disease patient-derived induced pluripotent stem cells free of viral reprogramming factors. Cell 2009;136:964–977.
20. Stadtfeld M, Nagaya M, Utikal J, *et al.* Induced pluripotent stem cells generated without viral integration. Science 2008;322:945–949.
21. Zhou W, Freed CR. Adenoviral gene delivery can reprogram human fibroblasts to induced pluripotent stem cells. Stem Cells 2009;27: 2667–2674.
22. Nishimura K, Sano M, Ohtaka M, *et al.* Development of defective and persistent Sendai virus vector: a unique gene delivery/expression system ideal for cell reprogramming. J Biol Chem 2011;286:4760–4771.
23. Okita K, Nakagawa M, Hyenjong H, *et al.* Generation of mouse induced pluripotent stem cells without viral vectors. Science 2008;322: 949–953.
24. Gonzales F, Monasterio MB, Tiscornia G, *et al.* Generation of mouse-induced pluripotent stem cells by transient expression of a single nonviral polycistronic vector. Proc Natl Acad Sci USA 2009; 106:8918–8922.
25. Jia F, Wilson KD, Sun N, *et al.* A nonviral minicircle vector for deriving human iPS cells. Nat Methods 2010;7:197–199.
26. Yu J, Hu K, Smuga-Otto K, *et al.* Human induced pluripotent stem cells free of vector and transgene sequences. Science 2009;324:797–801.
27. Kaji K, Norrby K, Paca A, *et al.* Virus-free induction of pluripotency and subsequent excision of reprogramming factors. Nature 2009;458: 771–775.
28. Woltjen K, Michael IP, Mohseni P, *et al.* PiggyBac transposition reprograms fibroblasts to induced pluripotent stem cells. Nature 2009; 458:766–770.
29. Yusa K, Rad R, Takeda J, *et al.* Generation of transgene-free induced pluripotent mouse stem cells by the piggyBac transposon. Nat Methods 2009;6:363–369.
30. Yakubov E, Rechavi G, Rozenblatt S, *et al.* Reprogramming of human fibroblasts to pluripotent stem cells using mRNA of four transcription factors. Biochem Biophys Res Commun 2010;394:189–193.
31. Kim D, Kim CH, Moon JI, *et al.* Generation of human induced pluripotent stem cells by direct delivery of reprogramming proteins. Cell Stem Cell 2009;4:472–476.
32. Zhou H, Wu S, Joo JY, *et al.* Generation of induced pluripotent stem cells using recombinant proteins. Cell Stem Cell 2009;4:381–384.
33. Miyoshi N, Ishii H, Nagano H, *et al.* Reprogramming of mouse and human cells to pluripotency using mature microRNAs. Cell Stem Cell 2011;8:633–638.
34. Hou P, Li Y, Zhang X, *et al.* Pluripotent stem cells induced from mouse somatic cells by small-molecule compounds. Science 2013;341: 651–654.
35. Gore A, Li Z, Fung HL, *et al.* Somatic coding mutations in human induced pluripotent stem cells. Nature 2011;471:63–67.
36. Toyoda M, Yamazaki-Inoue M, Itakura Y, *et al.* Lectin microarray analysis of pluripotent and multipotent stem cells. Genes Cells 2011; 16:1–11.

37. Nishino K, Toyoda M, Yamazaki-Inoue M, *et al.* Defining hypomethylated regions of stem cell-specific promoters in human iPS cells derived from extra-embryonic amnions and lung fibroblasts. PLoS One 2010;5:e13017.
38. Park IH, Zhao R, West JA, *et al.* Reprogramming of human somatic cells to pluripotency with defined factors. Nature 2008;451:141–146.
39. Hannan NR, Segeritz CP, Touboul T, *et al.* Production of hepatocyte-like cells from human pluripotent stem cells. Nat Protoc 2013;8:430–437.
40. Vallier L, Touboul T, Brown S, *et al.* Signaling pathways controlling pluripotency and early cell fate decisions of human induced pluripotent stem cells. Stem Cells 2009;27:2655–2666.
41. Pick M, Ronen D, Yanuka O, *et al.* Reprogramming of the MHC-I and its regulation by NFκB in human-induced pluripotent stem cells. Stem Cells 2012;30:2700–2708.
42. Marchand M, Anderson EK, Phadnis SM, *et al.* Concurrent generation of functional smooth muscle and endothelial cells via a vascular progenitor. Stem Cells Transl Med 2014;3:91–97.
43. Uosaki H, Fukushima H, Takeuchi A, *et al.* Efficient and scalable purification of cardiomyocytes from human embryonic and induced pluripotent stem cells by VCAM1 surface expression. PLoS One 2011;6:e23657.
44. Choi KD, Yu J, Smuga-Otto K, *et al.* Hematopoietic and endothelial differentiation of human induced pluripotent stem cells. Stem Cells 2009;27:559–567.
45. Cai J, DeLaForest A, Fisher J, *et al.* Protocol for directed differentiation of human pluripotent stem cells toward a hepatocyte fate, In: *StemBook(Internet)* 10 Jun 2012. Available fromhttp://www.ncbi.nlm.nih.gov/books/NBK133278.
46. Chambers SM, Fasano CA, Papapetrou EP, *et al.* Highly efficient neural conversion of human ES and iPS cells by dual inhibition of SMAD signaling. Nat Biotechnol 2009;27:275–280.
47. Lee G, Chambers SM, Tomishima MJ, *et al.* Derivation of neural crest cells from human pluripotent stem cells. Nat Protoc 2010;5:688–701.
48. Kriks S, Shim JW, Piao J, *et al.* Dopamine neurons derived from human ES cells efficiently engraft in animal models of Parkinson's disease. Nature 2011;480:547–551.
49. Di Giorgio FP, Boulting GL, Bobrowicz S, *et al.* Human embryonic stem cell-derived motor neurons are sensitive to the toxic effect of glial cells carrying an ALS-causing mutation. Cell Stem Cell 2008;3:637–648.
50. Lancaster MA, Renner M, Martin CA, *et al.* Cerebral organoids model human brain development and microcephaly. Nature 2013;501:373–379.
51. Nakano T, Ando S, Takata N, *et al.* Self-formation of optic cups and storable stratified neural retina from human ESCs. Cell Stem Cell 2012;10:771–785.
52. Suga H, Kadoshima T, Minaguchi M, *et al.* Self-formation of functional adenohypophysis in three-dimensional culture. Nature 2011;480:57–62.
53. Takebe T, Sekine K, Enomura M, *et al.* Vascularized and functional human liver from an iPSC-derived organ bud transplant. Nature 2013;499:481–484.
54. Melton DA. Using stem cells to study and possibly treat type 1 diabetes. Philos Trans R Soc Lond B Biol Sci 2011;366:2307–2311.
55. Matsunari H, Nagashima H, Watanabe M, *et al.* Blastocyst complementation generates exogenic pancreas *in vivo* in apancreatic cloned pigs. Proc Natl Acad Sci USA 2013;110:4557–4562.
56. Mahfouz MM, Li L, Shamimuzzaman M, *et al. De novo*-engineered transcription activator-like effector (TALE) hybrid nuclease with novel DNA binding specificity creates double-strand breaks. Proc Natl Acad Sci USA 2011;108:2623–2628.
57. Christian M, Cermak T, Doyle EL, *et al.* Targeting DNA double-strand breaks with TAL effector nucleases. Genetics 2010;186:757–761.
58. Hockemeyer D, Wang H, Kiani S, *et al.* Genetic engineering of human pluripotent cells using TALE nucleases. Nat Biotechnol 2011;29:731–734.
59. Tesson L, Usal C, Ménoret S, *et al.* Knockout rats generated by embryo microinjection of TALENs. Nat Biotechnol 2011;29:695–696.
60. Sander JD, Cade L, Khayter C, *et al.* Targeted gene disruption in somatic zebrafish cells using engineered TALENs. Nat Biotechnol 2011;29:697–698.
61. Sung YH, Baek IJ, Kim DH, *et al.* Knockout mice created by TALEN-mediated gene targeting. Nat Biotechnol 2013;31:23–24.
62. Pennisi E. The tale of the TALEs. Science 2012;338:1408–1411.
63. Ochiai H, Miyamoto T, Kanai A, *et al.* TALEN-mediated single-base-pair editing identification of an intergenic mutation upstream of BUB1B as causative of PCS (MVA) syndrome. Proc Natl Acad Sci USA 2014;111:1461–1466.
64. Bacman SR, Williams SL, Pinto M, *et al.* Specific elimination of mutant mitochondrial genomes in patient-derived cells by mitoTALENs. Nat Med 2013;19:1111–1113.
65. Kim Y, Kweon J, Kim A, *et al.* A library of TAL effector nucleases spanning the human genome. Nat Biotechnol 2013;31:251–258.
66. Liu J, Gaj T, Patterson JT, *et al.* Cell-penetrating peptide-mediated delivery of TALEN proteins via bioconjugation for genome engineering. PLoS One 2014;9:e85755.
67. Jia J, Jin Y, Bian T, *et al.* Bacterial delivery of TALEN proteins for human genome editing. PLoS One 2014;9:e91547.
68. Cong L, Ran FA, Cox D, *et al.* Multiplex genome engineering using CRISPR/Cas systems. Science 2013;339:819–823.
69. Mali P, Yang L, Esvelt KM, *et al.* RNA-guided human genome engineering via Cas9. Science 2013;339:823–826.
70. Jinek M, East A, Cheng A, *et al.* RNA-programmed genome editing in human cells. Elife 2013;2:e00471.
71. Cho SW, Kim S, Kim JM, *et al.* Targeted genome engineering in human cells with the Cas9 RNA-guided endonuclease. Nat Biotechnol 2013;31:230–232.
72. Hwang WY, Fu Y, Reyon D, *et al.* Efficient genome editing in zebrafish using a CRISPR-Cas system. Nat Biotechnol 2013;31:227–229.
73. Wang H, Yang H, Shivalila CS, *et al.* One-step generation of mice carrying mutations in multiple genes by CRISPR/Cas-mediated genome engineering. Cell 2013;153:910–918.
74. Wu Y, Liang D, Wang Y, *et al.* Correction of a genetic disease in mouse via use of CRISPR-Cas9. Cell Stem Cell 2013;13:659–662.
75. Shalem O, Sanjana NE, Hartenian E, *et al.* Genome-scale CRISPR-Cas9 knockout screening in human cells. Science 2014;343:84–87.
76. Wang T, Wei JJ, Sabatini DM, *et al.* Genetic screens in human cells using the CRISPR-Cas9 system. Science 2014;343:80–84.
77. Yin H, Xue W, Chen S, *et al.* Genome editing with Cas9 in adult mice corrects a disease mutation and phenotype. Nat Biotechnol 2014;32:551–553.
78. Chen B, Gilbert LA, Cimini BA, *et al.* Dynamic imaging of genomic loci in living human cells by an optimized CRISPR/Cas system. Cell 2013;155:1479–1491.
79. Qi LS, Larson MH, Gilbert LA, *et al.* Repurposing CRISPR as an RNA-guided platform for sequence-specific control of gene expression. Cell 2013;152:1173–1183.
80. Kearns NA, Genga RM, Enuameh MS, *et al.* Cas9 effector-mediated regulation of transcription and differentiation in human pluripotent stem cells. Development 2014;141:219–223.

Pigment Cell Melanoma Res. **27**; 1039–1050

ORIGINAL ARTICLE

A melanocyte–melanoma precursor niche in sweat glands of volar skin

Natsuko Okamoto[1,2*], Takahiro Aoto[1,*], Hisashi Uhara[3], Satoshi Yamazaki[4], Hidenori Akutsu[5], Akihiro Umezawa[5], Hiromitsu Nakauchi[4], Yoshiki Miyachi[2], Toshiaki Saida[3] and Emi K. Nishimura[1]

1 Department of Stem Cell Biology, Medical Research Institute, Tokyo Medical and Dental University, Tokyo, Japan **2** Department of Dermatology, Kyoto University Graduate School of Medicine, Kyoto, Japan **3** Department of Dermatology, Shinshu University School of Medicine, Matsumoto, Japan **4** Division of Stem Cell Therapy, Center for Stem Cell Biology and Medicine, Institute of Medical Science, University of Tokyo, Tokyo, Japan **5** Department of Reproductive Biology, National Research Institute for Child Health and Development, Tokyo, Japan

CORRESPONDENCE Emi K. Nishimura, e-mail: nishscm@tmd.ac.jp

*These authors contributed equally to this work.

KEYWORDS melanocyte stem cell/melanoma/sweat gland/niche

PUBLICATION DATA Received 15 June 2014, revised and accepted for publication 24 July 2014, published online 26 July 2014

doi: 10.1111/pcmr.12297

Summary

Determination of the niche for early-stage cancer remains a challenging issue. Melanoma is an aggressive cancer of the melanocyte lineage. Early melanoma cells are often found in the epidermis around sweat ducts of human volar skin, and the skin pigmentation pattern is an early diagnostic sign of acral melanoma. However, the niche for melanoma precursors has not been determined yet. Here, we report that the secretory portion (SP) of eccrine sweat glands provide an anatomical niche for melanocyte–melanoma precursor cells. Using lineage-tagged H2B-GFP reporter mice, we found that melanoblasts that colonize sweat glands during development are maintained in an immature, slow-cycling state but renew themselves in response to genomic stress and provide their differentiating progeny to the epidermis. FISH analysis of human acral melanoma expanding in the epidermis revealed that unpigmented melanoblasts with significant cyclin D1 gene amplification reside deep in the SP of particular sweat gland(s). These findings indicate that sweat glands maintain melanocyte–melanoma precursors in an immature state in the niche and explain the preferential distribution of early melanoma cells around sweat glands in human volar skin.

Introduction

Human cutaneous melanoma is a highly aggressive cancer that is resistant to traditional cancer treatments (Garbe et al., 2011; Mocellin et al., 2010; Wheatley, 2003). Acral (volar skin) melanoma is the most prevalent subtype of melanoma in the non-Caucasian population. Human volar skin of peripheral extremities is minimally exposed to UV sunlight and contains abundant eccrine sweat glands but no hair follicles as the main skin appendage (Curtin et al., 2005). The characteristic skin pigmentation pattern of acral melanoma can be recognized with a magnifying glass called a dermoscopy in a 'parallel ridge pattern', which reflects the preferential proliferation and differentiation of melanoma cells around sweat ducts (Oguchi et al., 1998; Saida, 2007; Saida et al., 2004, 2011). This method devised by Saida, one of the authors of this manuscript and his colleagues, has

Significance

Acral volar skin, which lacks hair follicles but contains abundant eccrine sweat glands, is highly susceptible to melanoma even without exposure to ultraviolet light. The dermoscopic pattern of parallel ridges has 99% specificity to detect acral melanomas, while the cause of the skin pigmentation pattern has been unknown. Our study is the first to identify sweat glands as the anatomical niche for melanocyte–melanoma precursor cells in mammalian volar skin.

enabled the accurate diagnosis with a 99% specificity (Saida et al., 2004) of early acral melanoma even as small as a few millimeter and has become the standard methodology for early diagnosis of melanoma in the volar skin nowadays. However, the origin of acral melanoma cells, the cause of the parallel ridge pattern, and even the existence of melanocytic cells in sweat glands have yet to be characterized. Recent reports on sweat gland-centric distribution of melanoma cells in some acral melanoma cases (Zembowicz and Kafanas, 2012) and repigmentation of the human white spot epidermis around sweat glands (Makino et al., 2013) have suggested the possibility that unknown melanocyte precursors (melanoblasts) exist in sweat glands. Thus, the skin appendage may provide a niche or special microenvironment not only for melanoblasts but also for earliest melanoma cells.

In most somatic stem cell systems, stem cells are maintained in an immature and quiescent state but become activated to undergo self-renewal to provide amplifying and differentiating progeny for tissue homeostasis (Fuchs et al., 2004; Li and Clevers, 2010). We previously identified melanocyte stem cells (McSCs) in the bulge/sub-bulge area of murine and human hair follicles and reported that the niche plays a dominant role in stem cell fate determination (Nishimura et al., 2002, 2005). The McSCs self-renew and provide their progeny not only to the hair bulb for hair pigmentation in physiological condition but also to the surrounding epidermis for skin pigmentation (Nishimura et al., 2002). During the process of epidermal repigmentation, the repigmented spots often start from the orifice of hair follicles with contiguous distribution of melanoblasts/melanocytes in the upper outer root sheath starting from the hair follicle bulge to the epidermal basal layer (Nishimura, 2011; Nishimura et al., 2002). It is thus possible that sweat glands also provide similar niche microenvironment not only for normal melanoblasts but also for early melanoma cells.

In this paper, we hypothesized that dormant immature melanocyte–melanoma precursors exist in mammalian eccrine sweat glands, which are abundantly distributed on the volar skin. We searched for the population by taking advantage of stable lineage tagging system, and we report here that such melanocyte–melanoma precursors exist in sweat glands of mammalian volar skin.

Results

To compare the architecture and pigmentation pattern of human and mouse volar skin, we first performed histological analysis. As shown in Figure 1A–C, both human and mouse volar skin were characterized by a similar thickened epidermis with rete ridges extending into the underlying dermis and by the abundant presence of sweat glands (Figure 1A–C). No pigment-containing cells or melanocytic marker-expressing cells were detectable with conventional immunohistochemistry in the sweat glands found in the footpads of non-aged adult C57/BL6Cr mice (Figure 1D). In contrast, some pigment-containing cells were found in the sweat glands and the overlying epidermis from 2-year-old mice (Figure 1E and data not shown), which suggested that unpigmented melanoblasts that correspond to melanocyte stem cells or progenitors exist in non-hair-bearing volar skin. *Dct-lacZ* transgene (Figure 1F) and endogenous Dct protein expression, which has been used for melanocyte lineage tagging including melanocyte stem cells (McSCs) in hair follicles (Mackenzie et al., 1997; Nishimura et al., 2002), failed to tag that cell population in adult footpad skin (Figure 1H and data not shown). Thus, we examined the developmental process of melanocytes in the distal hindlimb using Dct-lacZ and expression of endogenous Dct as markers for melanoblasts. As shown in Figure 1G and Figure S1–S3, we succeeded in chronologically analyzing the distribution of migrating melanoblasts, which first appear in the developing dermis, then in the epidermis, and finally in the sweat buds, and of their eventual colonization in mature sweat glands in volar skin. This suggested that melanoblasts that colonize the sweat glands during development are maintained in a dormant and immature state with profound downregulation of lineage markers after development until they are reactivated during the physiological aging process.

Follicular McSCs, which reside in the bulge/sub-bulge area of hair follicles, are maintained in a quiescent, inactivated state during the hair cycle except for their activation for their self-renewal at the anagen growth phase (Nishimura et al., 2002, 2005, 2010). Upon genotoxic stress or aging, the follicular McSCs ectopically differentiate within the stem cell niche without renewing themselves (Inomata et al., 2009). We hypothesized that dormant immature melanoblasts that respond to aging and/or genotoxic stress exist in the sweat glands and generate mature melanocytes. To test this, we irradiated young *Dct-lacZ* transgenic (tg) mice and searched for melanocytic cells in mouse volar skin. Melanin-containing mature melanocytes appeared in sweat glands of the mouse volar skin within a week after 5 Gy ionizing irradiation (IR) (Figure 1K) and persisted for more than a month (Figure 1L, M), while those cells were only occasionally found in non-irradiated control skin (data not shown). As DNA damage accumulates in long-lived stem cells during aging (Nijnik et al., 2007; Rossi et al., 2007; Ruzankina et al., 2007), the above phenomenon induced by IR and the similar phenomenon associated with aging (shown in Figure 1E, I) suggest that both aging and genotoxic stress stimulate a putative stem/precursor cell population to supply pigment-producing melanocytes to the epidermis through the dermal-epidermal ducts in acral volar skin.

To identify putative stem/precursor cells which would explain the above phenomena, we developed *Dct-H2B-GFP* transgenic mice, in which non-dividing/slow-cycling melanocytic cells stably retain the expression of histone-GFP

fusion protein under control of the *Dct* promoter with the LCR element once the promoter is activated (Figure 1N and Figure S4A) (Ganss et al., 1994; Mackenzie et al., 1997; Kanda et al., 1998). As shown in Figure S4B–Y, all known melanocyte lineage cells can be efficiently tagged using GFP in these transgenic mice. The distribution pattern of GFP expressing cells was identical with that of *lacZ* expressing cells in *Dct-lacZ* transgenic mice during development (Figure S4B–J). In mouse volar skin, GFP$^+$ melanoblasts appear in the epidermis by embryonic day (E) 17.5 (Figure 1O, U), then migrate down into the epidermal buds, and finally colonize the tip of immature sweat glands (Figure 1P–R, U). This area then develops into the secretory portion (SP) of the sweat gland (Figure 1S, T). Similar migration processes were observed with *Dct-lacZ* transgenic mice (data not shown).

To identify the population which just colonizes the SP of sweat glands, we analyzed footpads of neonatal mice. The GFP$^+$ melanoblasts in sweat glands are located well inside the basement membrane and are surrounded by K8$^+$ luminal keratinocytes and underlying SMA$^+$K5$^+$ myoepithelial cells (Figure 2A–C). These GFP$^+$ cells in the neonatal skin express melanocyte lineage marker proteins such as Mitf and Pax3 (Figure 2I, K) and downstream target genes of Mitf including Dct, tyrosinase-related protein 1 (Trp1), tyrosinase (Tyr), and Silv/Pmel17 (Figure 2D–F and data not shown), but none of the following non-melanogenic cell markers tested including Nestin (a neural

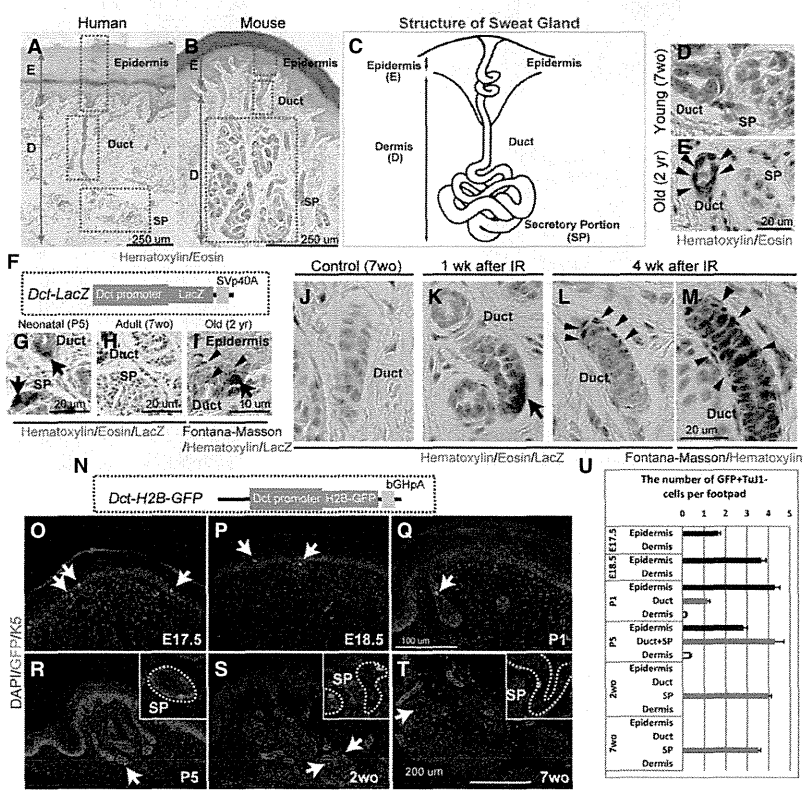

Figure 1. The existence of melanocytic sources in human and mouse sweat glands of acral skin. (A, B) Organization of eccrine sweat glands in mouse and human acral skin. The hematoxylin-eosin-stained sections are from human finger skin (A) and mouse footpad skin (B). (C) Schematic diagram of a sweat gland. The structure is similar both in mice and in humans. (D, E) Hematoxylin-eosin-stained sections of footpad skin of 7-week-old (7wo) (young) (D) and 2-year-old (2 yr) (old) (E) mice). Melanin-containing cells are observed in the sweat duct, but not in the secretory portion (SP), of 2-year-old mice (arrowheads). (F) Structure of the LacZ reporter under control of the melanocyte-specific Dct promoter (Dct-LacZ). (G–I) LacZ-stained skin of the footpad of *Dct-LacZ* tg mice [G; 5 day old (P5), H; 7 week old (7wo) and I; 2 year old (2yo)]. LacZ$^+$ melanocytic cells are found in the sweat duct and SP at P5 mice (arrows) and old mice, while no LacZ$^+$ cells are detectable at 7wo (H). (J–L) LacZ-stained skin of the footpad of 5 Gy-irradiated *Dct-LacZ* tg mice. Dct-LacZ$^+$ cells (arrow) appear in the sweat duct at 1 week (1 wk) after IR (K), and melanin-containing cells (arrowheads) appear in the sweat duct at 4 weeks (4 wk) after IR (L). (J–M) stained with hematoxylin-eosin, (M) Fontana-Masson staining for the detection of melanin. (N) Structure of the H2B-GFP reporter under control of the melanocyte-specific Dct promoter and the LCR element (Dct-H2B-GFP). (O–T), Distribution of H2B-GFP expressing cells in the developing footpad skin of *Dct-H2B-GFP* tg mice at different stages. GFP$^+$ cells migrating from the epidermis (green: arrows) toward the SP (the area encircled by the dotted line) of glands. Keratin 5$^+$ myoepithelial/basal keratinocyte immunostaining (red) defines the gland structure. GFP$^+$ cells are found in the epidermis at E17.5 (O) and subsequently in the sweat gland primordial buds at E18.5 (P). At postnatal day (P) 1 (Q), GFP$^+$ cells are found in the developing ducts. The majority of GFP$^+$ cells are settled in the SP of glands between P5 (R), 2 weeks old (2wo) (S) and 7 weeks old (7wo) (T) after birth. Nuclei are counterstained with DAPI (blue). The insets show magnified images of GFP expressing cells. (U) The distribution and number of GFP$^+$TuJ1$^-$ cells in the acral skin of each developmental stage. n = 3 mice each genotypes. Error bars represent SD of three independent experiments. Statistical significance at the level of $P < 0.01$.

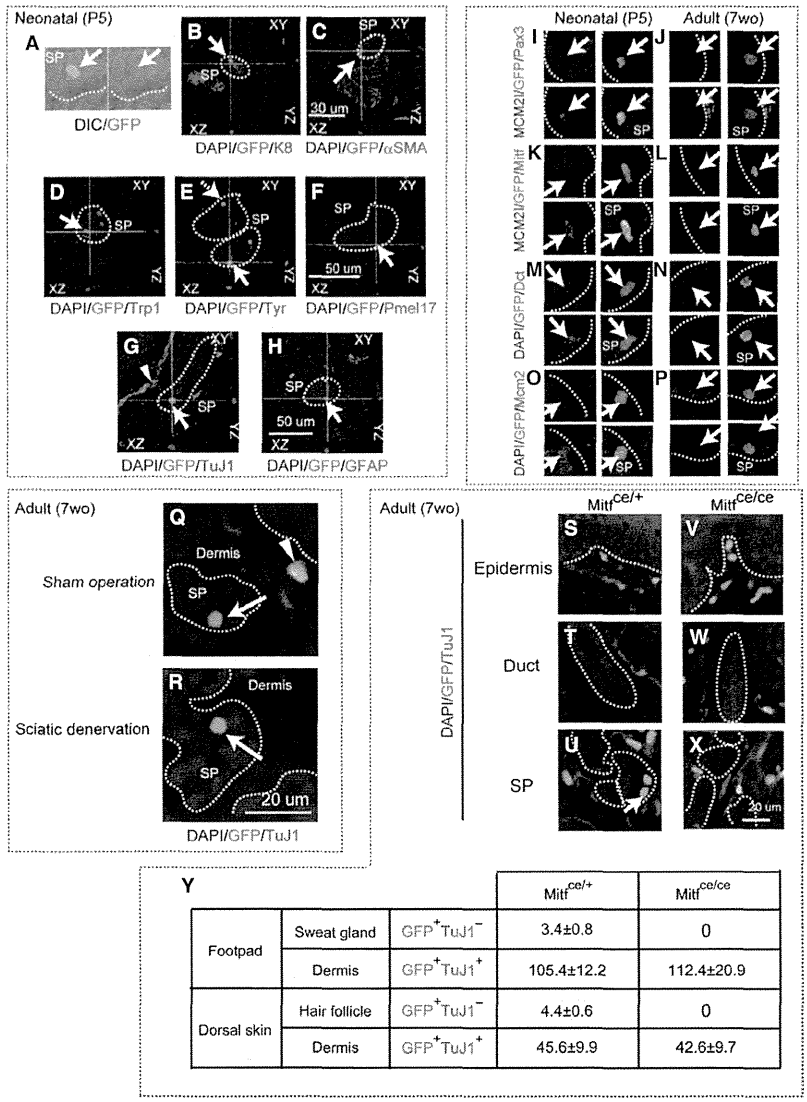

Y

			Mitf$^{ce/+}$	Mitf$^{ce/ce}$
Footpad	Sweat gland	GFP$^+$TuJ1$^-$	3.4±0.8	0
	Dermis	GFP$^+$TuJ1$^+$	105.4±12.2	112.4±20.9
Dorsal skin	Hair follicle	GFP$^+$TuJ1$^-$	4.4±0.6	0
	Dermis	GFP$^+$TuJ1$^+$	45.6±9.9	42.6±9.7

Figure 2. Identification of slow-cycling melanoblasts located in the SP of sweat glands in acral skin using *Dct-H2B-GFP* transgenic (tg) mice. (A) GFP$^+$ cells (green) in the SP (the area encircled by the dotted line) are melanin rounded cells as shown in DIC image. (A–H) Confocal analysis of GFP and immunostaining of various lineage markers performed on P5 footpad sections of *Dct-H2B-GFP* tg mice. (B, C) GFP$^+$ cells (green) are located between keratin 8$^+$ glandular cells (red) (B) and α-SMA$^+$ myoepithelial cells (red)(C). GFP$^+$ cells in the developing SP (the area encircled by the dotted line) of glands co-express melanosomal proteins, TRP1 (D), TYR (E) and Pmel17/Silv (F) but not TuJ1 (G) or GFAP (H). TYR immature GFP$^+$ cells were also occasionally found in the SP (E, dotted arrow). Nuclei are counterstained with DAPI (blue). (I–P) expression of GFP and various cell markers in the SP at P5 and 7wo. Downregulation of the lineage markers Pax3, Mitf, or Dct was observed in GFP$^+$ melanoblasts in the SP of adult mice (I–N). GFP$^+$ melanoblasts were kept in an MCM2 quiescent state in the adult stage (J, L, P). (Q, R) The number of GFP$^+$TuJ1$^+$ cells (arrowhead) in the dermis was profoundly reduced after sciatic denervation, while GFP$^+$TuJ1 cells (arrows) were maintained in the SP. (S, X) Immunostaining of the footpad sections of 7wo *Mitf$^{ce/+}$; Dct-H2B-GFP$^{tg/+}$* (S–U), and *Mitf$^{ce/ce}$;Dct-H2B-GFP$^{tg/+}$* (V–X) mice for GFP and TuJ1 expression. GFP$^+$TuJ1 melanocytes (arrows) were found in the SP of *Mitf$^{ce/+}$*, but not in *Mitf$^{ce/ce}$* mice. GFP$^+$TuJ1$^+$ neurons exist outside of the glands in both types of mice. (Y) The average number of GFP$^+$TuJ1 melanoblasts per gland in a single footpad and per single hair follicles and of the dermal GFP$^+$TuJ1$^+$ cells (per single footpad skin and per 1 mm width of dorsal skin) at 7 weeks in *Mitf$^{ce/+}$;Dct-H2B-GFP $^{tg/+}$*, and *Mitf$^{ce/ce}$;Dct-H2B-GFP $^{tg/+}$* mice.

progenitor marker), p75 (a neural crest progenitor marker), TuJ1 and Pgp9.5 (a peripheral nerve marker), GFAP and MPZ (Schwann cell markers), and keratin 20 (a Merkel cell marker) (Figure 2G, H, Figure S2 and data not shown). Furthermore, no significantly close association between these GFP$^+$ melanoblasts that express melano-

genic genes including Dct protein during development with TuJ1$^+$ non-melanocytic cells in the dermis has been found during the earlier developmental processes (Figure S1–S3 and data not shown). These data indicate that GFP$^+$ cells that migrated from the epidermis into the developing sweat glands are melanocyte lineage cells.

Next, we examined the transition of the GFP$^+$ cell state after the neonatal stage. GFP$^+$ melanoblasts are maintained in an immature unpigmented state in the SP with drastic downregulated expression of global melanogenic genes including Pax3 and Mitf and its downstream genes such as Dct, Dct-lacZ, and Tyr by 7 weeks after development without differentiating into mature melanocytes (Figure 2I–N). At the same time, they lose expression of Mcm2, a marker for the non-Go cell state(Kingsbury et al., 2005) after the neonatal stage, indicating that these cells go into the quiescent, inactivated state after development (Figure 2O, P). It is notable that McSCs that reside in the hair follicle bulge also downregulate expression of Dct-lacZ and melanogenic genes when they enter the quiescent state (Nishimura et al., 2010) while maintaining high levels of GFP expression throughout the hair cycle (Figure S4 and data not shown). Thus, we concluded that melanoblasts are maintained in an immature inactivated state in the lower sweat glands after development similar to McSCs in the hair follicle bulge area.

The other GFP$^+$ population distinguished from the melanocyte lineage in acral volar skin is the TuJ1-expressing GFP$^+$ cell population in the dermis outside of sweat glands (Figure 2G, arrowhead). Most of these cells appear at around prenatal stage in the dermis (data not shown) and co-express the neuronal markers TuJ1 and less frequently Pgp9.5, but not Nestin, mature Schwann cell markers such as GFAP and MPZ/P0 nor the neural crest progenitor marker, p75 (Figure 2G, H, Figure S5 and data not shown). To confirm the identity of these dermal GFP$^+$ cells, we performed sciatic denervation. As shown in Figure 2Q, R, the GFP$^+$TuJ1$^+$ cells disappeared from the dermis, suggesting that the dermal GFP$^+$ cells are peripheral neurons or associated neuron-dependent precursor cells (Figure 2Q, R and Figure S6). Then, we analyzed *Mitf$^{ce/ce}$* mutant mice which specifically lack melanocyte lineage cells (Steingrimsson et al., 1994; Zimring et al., 1996). We found that *Mitf$^{ce/ce}$* mice with the GFP reporter transgene lack GFP$^+$ cells in the sweat glands (Figure 2S–Y). On the other hand, GFP$^+$TuJ1$^+$ cells are maintained in the dermis with neuronal morphology in *Mitf$^{ce/ce}$* mice as well, demonstrating that the GFP$^+$ cells in the dermis are non-melanocytic cells. To further confirm the lineage identity of GFP$^+$ cells in the sweat glands, we took advantage of ACK2, a neutralizing antibody against Kit (c-Kit), which has been used to deplete amplifying melanoblasts in developing skin (Nishimura et al., 2002). ACK2 treatment of the neonatal skin depleted almost all GFP$^+$ cells in sweat glands (Figure 3A, B and Figure S7), while ACK2 treatment after the neonatal stage, such as 7 weeks after birth, did not deplete GFP$^+$ cells in the sweat glands (Figure 3B). This demonstrates that the glandular GFP$^+$ cells are *bona fide* melanoblasts which develop in Kit-dependent manner but become inactivated to go into the quiescent and immature state after the neonatal stage and survive in a Kit-independent manner similar to slow-cycling McSCs in hair follicles (Nishimura et al., 2002).

Self-renewal and quiescence are important features of somatic stem cells including hair follicle McSCs (Cotsar-

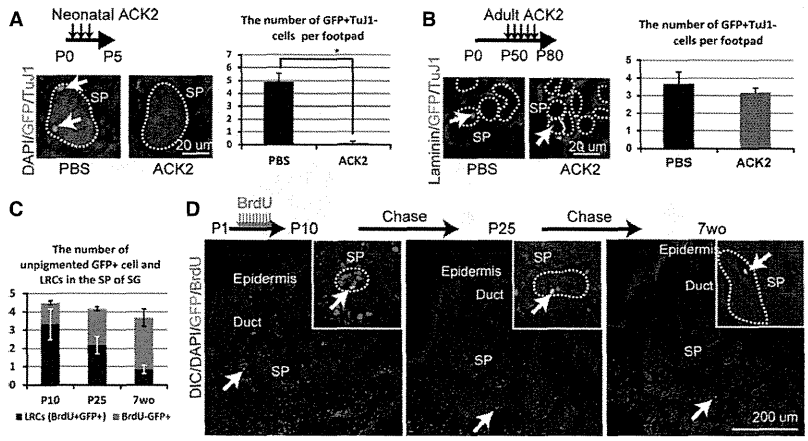

Figure 3. Dct-H2B-GFP$^+$ cells are slow cycling, ACK2-resistant melanoblasts in adult skin. (A, B) The differential ACK2 sensitivity of GFP$^+$TuJ1 cells in sweat glands after ACK2 administration at the neonatal (A) or the adult stage (B). The number of GFP$^+$TuJ1 cells in the SP is shown. A, While GFP$^+$TuJ1 cells are found in the SP of control mice (green; arrows), almost no GFP$^+$TuJ1 cells remain in the SP of neonatal ACK2-treated mice. B, GFP$^+$TuJ1 cells remain in the SP of adult ACK2-treated mice. Error bars represent SD of three independent experiments. *, statistical significance at the level of $P < 0.01$. (C, D) Pulse-chase experiments with BrdU in *Dct-H2B-GFP* tg mice. The total number of GFP$^+$TuJ1 cells in the SP did not significantly change from post-neonatal (P10) to adult stage (7wo) (C). After continuous BrdU injection (P1–P10), almost all cells in the acral skin of *Dct-H2B-GFP* tg mice were labeled with BrdU at P10 (D; arrows (SP)). At P25 and 7wo, GFP$^+$ melanoblasts were found exclusively in the SP of sweat glands with significant retention of BrdU (D). The label is still retained in some GFP$^+$ melanoblasts at 7wo (D; arrows and C). The insets show magnified images of GFP expressing cells.

elis et al., 1990; Fuchs et al., 2004; Nishimura et al., 2002). To examine whether the GFP$^+$ cells identified here are slow-cycling cells or quiescent cells, we performed pulse-chase experiments with BrdU using our transgenic mice. As shown in Figure 3C, D, we found that GFP$^+$ cells in sweat glands are able to retain the BrdU label for more than a month, while most other cells in volar skin lost their BrdU label earlier. The BrdU retention level was stably high in the majority of GFP$^+$ melanoblasts at P25 but became steadily diluted in a subset of them at P50 and was further diluted to barely detectable levels at P100 (Figure 3C, D and Figure S8). Adjacent GFP$^+$ cells, which show an almost identical dilution level, were also found at P50 (7wo) and show unpigmented immature cell bodies

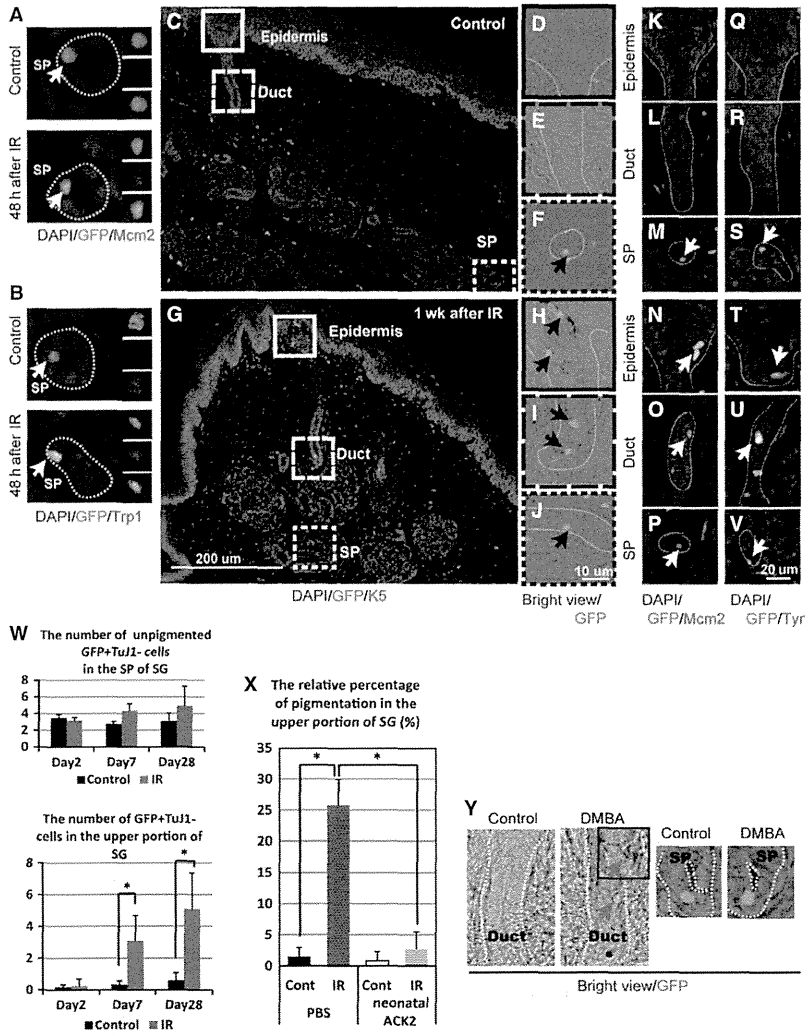

Figure 4. Melanoblasts in the SP of sweat glands maintain themselves and provide proliferating and differentiating melanocytes to the epidermis in response to IR or oncogenic stress. (A, B) Transient cell cycle entry and commitment of GFP$^+$ cells in the SP. At around 48 hr after IR, expression of MCM2 and TRP1 was found transiently in some GFP$^+$ cells located within the SP (arrow). (C–V) Behavior of GFP$^+$ cells in sweat glands after 5 Gy IR. Immunostaining for keratin 5 (K5) was performed on footpad skin sections in *Dct-H2B-GFP* tg mice to chase GFP$^+$ cells (green) located within the glands after IR. While no GFP$^+$ cells exist in the duct or the epidermis in control mice (C–F), GFP$^+$ cells (arrows) exist in the dermal-epidermal duct and the epidermis after IR at 1 week (1 wk) (G–J). Bright view images merged with GFP images are shown for the epidermis (solid-line square) (D, H), the sweat duct (marked by the long-dashed line square) (E, I), and SP (the short-dashed line square) (F, J) on the right side of the large panel. Melanogenesis can be observed only in the duct or in the epidermis (H, I). K–P and Q–V, MCM2, and TYR immunostaining images are shown, respectively, on the right side of the figure. Most GFP$^+$ cells (arrows) at the SP are MCM2- (M, P), while IR-induced ductal or epidermal GFP$^+$ melanocytes (arrows) are MCM2$^+$ (red) (N, O) and TYR$^+$ (red) (T, U). (W) The number of GFP$^+$ cells located in the SP remained stable after IR (graph in the upper column), while the number of GFP$^+$ cells located within the duct of glands after IR was significantly increased (graph in the lower column). *, statistical significance at the level of $P < 0.05$. (X) IR-induced pigmentation of the upper portions of glands after IR was dramatically impaired when mice were pretreated with ACK2 at the neonatal stage. Error bars represent SD of three independent experiments. *, statistical significance at the level of $P < 0.01$. Nuclei are counterstained with DAPI (blue). (Y) Pigmented GFP$^+$ cells (red arrow) were found in the duct at 4 weeks after DMBA, while GFP$^+$ cells in the SP were kept in an unpigmented state.

(Figure S8). Only a few unpigmented GFP$^+$ cells reside in the SP in each footpad (Figure 3D) and maintained well from the neonatal to the adult stage (Figure 3C). Most of these unpigmented GFP$^+$ melanoblasts are usually negative for the non-Go cell state marker Mcm2 and Ki67 after development (Figure 2O, P and data not shown). Therefore, these data collectively indicate that the GFP$^+$ immature melanoblasts are an extremely rare population in tissues and are normally kept in a quiescent state after development but occasionally undergo self-renewal in the SP of the sweat glands even under normal physiological conditions. As mice that congenitally lack melanocyte lineage cells (Cable et al., 1995) are able to sweat from the footpads (Figure S9) and maintain the integrity of sweat glands (Figure 2S–X and data not shown), we assumed that the glandular melanoblasts in the SP may not be essential for the homeostasis and sweating function of sweat glands but could become pathogenic when abnormally activated.

We then determined whether the quiescent GFP$^+$ cells were able to generate pigmented melanocytes upon activation. As aged sweat glands occasionally contain pigmented melanocytes with γ-H2AX foci formation outside of the niche (data not shown), we hypothesized that melanocyte precursors are transiently activated to respond to endogenous or exogenous genomic stress during aging. To test this, we performed chronological analysis for the fate of GFP$^+$ melanoblasts after 5 Gy IR. GFP$^+$ cells in the SP showed transient expression of Mcm2, a marker for the non-Go state (Kingsbury et al., 2005) (13.3 ± 4.7% in irradiated mice versus 0% of control mice [n = 3]) (Figure 4A) and melanogenic genes such as Trp1 (6.3 ± 4.5% in irradiated mice versus 0% of control mice [n = 3]) at 48 h after IR (Figure 4B). Subse-

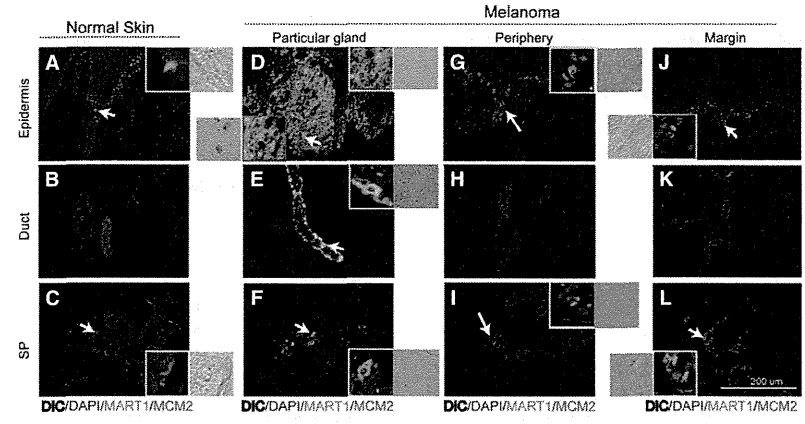

M

	Sample	Age/Sex	Size (mm)	Thickness (mm)	Epidermis: Furrow Area (CPL)	Epidermis: Ridge Area (CPI)	Duct: particular gland	Duct: others	Secretory Portion: particular gland	Secretory Portion: others
Normal Skin	A	32/F	-	-	–	+	–		+	
	B	62/F	-	-	–	+	–		–	
	C	51/F	-	-	–	+	–		+	
Melanoma	D	78/F	23x23	in situ	+	++	–	–	+	+
	E	56/F	20x12	in situ	+	++	+	–	+	+
	F	79/F	15x15	in situ	+++	+++	++	–	+	+
	G	95/M	70x30	0.9	+	++	++	–	+	+
	H	93/F	33x30	3.2	+	+++	+	–	+	+

CPL, crista profunda limitans; CPI,crista profunda intermidia
–, no MART1+ cell in 10 sections; +, 1-3 MART1+ cells in 10 sections; ++, 3-10 MART1+ cells in 10 sections; +++, more than 10 MART1+ cells in 10 sections; red, MCM2+MART1+ cells.

Figure 5. Identification of melanoblasts in the SP of human volar sweat glands as an expandable source of early acral melanoma. (A–L) Localization of melanocyte/melanoma cells and their cell cycle status in human volar sweat glands. Human normal volar skin (A–C) and early melanoma skin (D–L) were immunostained for the lineage markers, MART1 (shown in green) and MCM2 (in red). A small number of MART1$^+$MCM2 cells were found in the epidermis close to the sweat duct within the ridge area of the skin (A) and the SP (C), but not within the duct (B). (D) A nest of MART1$^+$MCM2$^+$ unpigmented melanoma cells (white arrows) and MART1$^+$MCM2^{low} pigmented melanoma cells (red arrows) was found in the epidermis of the ridge area of the lesional skin of melanoma *in situ*. MART1$^+$ cells are aligned contiguously throughout the duct (arrow; E) and SP (arrow; F) area of a particular sweat gland within the center of the lesion. At the periphery of the lesion, MART1$^+$MCM2$^+$ cells were found in the epidermis (arrow; G), but not in sweat glands (arrow; I). At the intact margin, there are MART1$^+$MCM2 melanoblasts, but no MART1$^+$MCM2$^+$ cells in the epidermis (J). The SP of an identical gland contains a MART1$^+$MCM2 melanoblast (L). Note that MART1$^+$ cells were found in the duct of particular glands at the lesion, but not in the surrounding glands at the margin of the lesion (H and K). Magnified images of MART1$^+$ cells are shown in the insets. Nuclei are counterstained with DAPI. (M) Table showing the distribution and proliferative status of MART1$^+$ cells in human acral skin samples. In normal control skin samples, a small number of MART1$^+$ cells were found in the SP and most of them are MCM2 , while those in early melanoma lesions are MCM2$^+$ and MART1$^+$MCM2$^+$ proliferative cells were found in the sweat duct and SP of particular glands.

quently, pigmented GFP$^+$ melanocytes appeared within the sweat ducts of a particular gland(s) and then in the surrounding epidermis within a week after IR (Figure 4G–I, W, and X), while the unpigmented GFP$^+$ cells were maintained in the SP (Figure 4C, F, G, J, and W). Importantly, the GFP$^+$ cells in the SP went back to the quiescent state with downregulation of these genes within a few days and were maintained again in an immature, unpigmented state within the niche (Figure 4J, P, and V). Those stem/precursor cell progeny generate melanin pigment by expressing melanogenic enzymes such as Tyr which is critical for melanin pigment synthesis (Figure 4T, U). As only a few GFP$^+$ cells reside in the SP in each footpad and are stably maintained (Figure 4W), these data indicate that the GFP$^+$ cells in the SP maintain themselves in an immature state and at the same time provide amplifying and differentiating progeny which migrate up into the epidermis through the sweat ducts. Therefore, the GFP$^+$ melanoblasts in the SP show the features of adult stem cells (Potten and Loeffler, 1990), and we named the population as McSCs in sweat glands.

As the GFP$^+$ McSCs reside in the SP, having direct contact with K8$^+$ luminal cells and SMA$^+$ myoepithelial cells within the SP of sweat glands (Figure 2B, C), we assumed that the SP serves as the anatomical niche for McSCs. To exclude the involvement or contribution of GFP$^+$TuJ1$^+$ neuronal cell lineages for skin pigmentation, we performed sciatic denervation prior to IR. As shown in Figure S6, irradiated GFP$^+$ cells in the SP are able to maintain and renew themselves and are also able to generate differentiated progeny even in the absence of neuronal cells in the dermis. Furthermore, when GFP$^+$ cells in the SP are depleted by administration of ACK2 at the neonatal stage, mature pigmented melanocytes did not appear in the sweat glands or in the epidermis of adult acral skin even after 5 Gy IR (Figure 4X, Figure S7, and data not shown), underlining the regenerating capability of the McSCs and their contribution to skin pigmentation.

Oncogenic stimuli such as exposure to carcinogens/mutagens and genetic alterations involved in human melanoma induce melanoma formation in mice (Larue and Beermann, 2007; Walker et al., 2011). We tested whether carcinogens also activate McSCs. As shown in Figure 4Y, DMBA application on mouse footpads also induced the appearance of pigmented GFP$^+$ cells in sweat glands. These data clearly demonstrate that MsSCs provide their pigmented progeny with the upper sweat glands in response to oncogenic or other genotoxic stimuli.

We searched for a similar McSC-like population in human acral volar skin using immunohistochemical staining with increased sensitivity (Figure S10). As shown in Figure 5, we detected MART1$^+$ unpigmented melanoblasts, which are located specifically in the SP of human sweat glands (Figure 5C and Figure S11C, F). Expression of other melanogenic genes (Figure S12 and S13) and MCM2 were not detectable in those cells in the adult skin (Figure 5C and data not shown). We also searched for a similar population in the sweat glands of non-volar skin areas such as the face and abdomen, but such melanoblasts were undetectable in those areas (data not shown). These data indicate that the population resides preferentially in the sweat glands of volar skin, at least in physiological conditions, and these immature and quiescent melanoblasts are most likely to be human McSC-like precursor cells.

Human acral skin forms a ridge and furrow pattern on the surface. Early acral melanoma shows preferential proliferation/pigmentation in the 'ridge epidermis', which corresponds to crista profunda intermedia (CPI) situated under the surface ridge and contains sweat ducts in the middle of the CPI in human acral epidermis. To address the possibility that human melanoma precursors reside in the sweat glands of acral skin, we selected cases in which the skin sections cover the whole sweat gland structure and analyzed the distribution of melanocyte lineage cells in human acral melanoma (n = 5) and in normal skin (n = 3). We found that MART1$^+$ unpigmented melanoblasts in the SP are increased in number with co-expression of MCM2 in the specific sweat gland(s) of the melanoma *in situ* lesion, which suggests that the McSC-like cells in those particular sweat glands are renewing themselves. These MART1$^+$ proliferating cells are found in the duct as well, which connects the SP to the 'ridge epidermis' of the lesional epidermis (Figure 5D–F, M samples D–F), suggesting that MART1$^+$ cells in the SP are providing melanocytic progeny to the duct and the epidermis similarly to mouse activated McSCl progeny. Notably, these lower-positioned MART1$^+$MCM2$^+$ cells in the SP and the lower duct are unpigmented, relatively small and bipolar in morphology (Figure 5F), while those located in the upper duct or in the lesional epidermis are larger, dendritic, and often pigmented (Figure 5D, E). This suggests that these abnormally proliferating cells in the lower part of sweat glands are maintained in an immature state in the special microenvironment but keep providing amplifying and differentiating melanoma cells to the epidermis. Importantly, MART1$^+$MCM2$^+$ cells are distributed contiguously or sparsely from the SP to the ridge epidermis only in particular sweat gland(s) but not in other surrounding glands in the lesion (Figure 5D–L). We examined 10 serial sections for each early melanoma originally evaluated as melanoma *in situ* (Figure 5M, samples D–F) and more advanced melanoma (samples G and H). Each case of early acral melanoma possesses at least one sweat gland, which contains proliferating MART1$^+$ cells distributed in the sweat gland starting from the SP to the intra-epidermal duct within the lesion (Figure 5D–F and M). Although it is believed that the distribution of early acral melanoma cells is limited within the epidermis ('*in situ*'), we found their scattered or contiguous distribution in some sweat glands. Importantly, the SP and the duct of other surrounding sweat

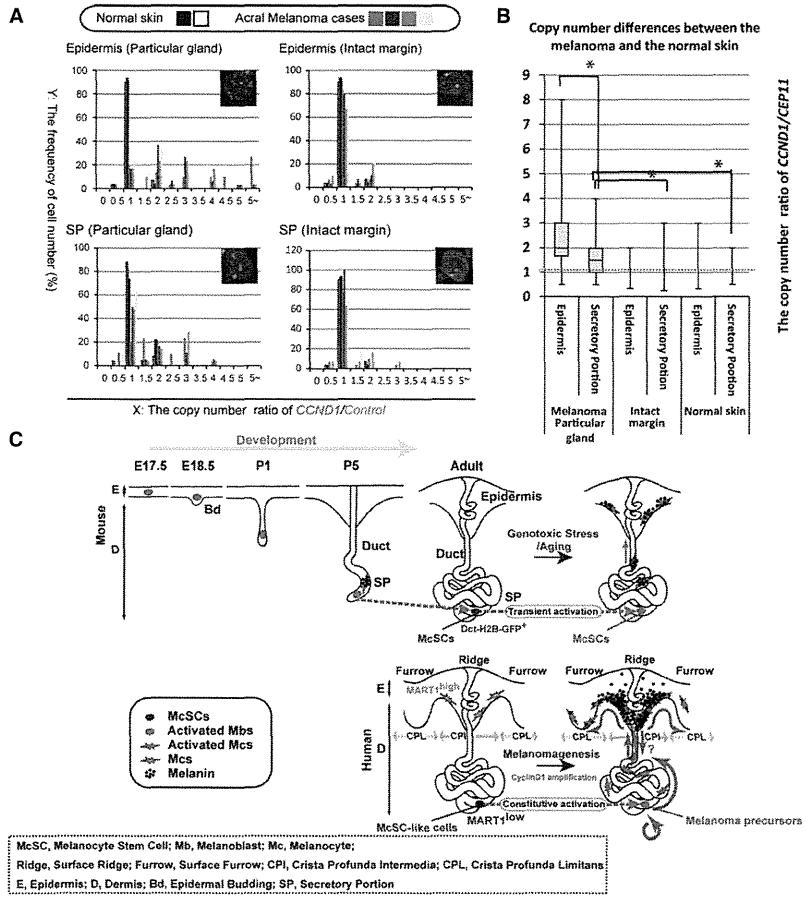

Figure 6. *CCND1* gene amplification in the SP within a melanoma lesion and a schematic for McSc (mice) or McSC-like cell (human) development, maintenance, and melanomagenesis. (A) Histograms showing the distribution of copy number variation of 11q13 *CCND1* genomic regions in the tumor center of early acral melanomas. Colored bars (red, blue, green, and yellow) show individual samples derived from acral melanoma cases, while colored bars (black and white) show control normal samples. The *Cep11* centromeric region was used to normalize the number of FISH signals between cells at different cell cycle stages. (B) Box plot showing the copy number differences between the epidermis and SP from melanoma and normal skin. Copy number amplification of the *CCND1* gene is found in the SP of sweat glands within the lesion but not in the normal skin and is significantly lower than that seen in the epidermis. *, statistical significance at the level of $P < 0.05$. (C) The fate and behavior of melanocyte lineage cells in sweat glands are summarized and combined with a hypothetical schematic for melanoma initiation from McSCs. Proliferating melanoblasts (red) that colonized the SP of the sweat glands enter a quiescent (Go) state just after development and become McSCs maintained in a dormant state (blue). These cells are activated transiently by extrinsic or intrinsic stresses such as genotoxic stress and during the normal aging process. Conversely, the corresponding population in the SP maintains its immaturity and cycling activity to renew the population and to generate their amplifying progenies which acquire further genetic alterations during their migration and maturation into noticeable melanoma cells in the epidermis.

glands are often not colonized by $MART1^{+}MCM2^{+}$ cells. Considering the features of mouse sweat gland McSCs, these findings suggest that human sweat gland melanocyte precursors are also only transiently activated for their renewal upon a stress but are able to generate abnormal melanocyte–melanoma precursors which keep proliferating in the niche in particular sweat glands during aging. As the structure of these sweat glands is well maintained, the cycling precursors in the SP are most likely to keep generating their amplifying progeny which migrate toward the epidermis where they mature into histologically recognizable melanoma cells and spread horizontally within the epidermis with some colonization preference to the ridge epidermis in early acral melanoma (Figure S14).

CCND1 gene amplification has been found in 23.8–44.4% of early acral melanoma cases (North et al., 2008; Sauter et al., 2002; Takata et al., 2005), yet the exact distribution of the *CCND1*-amplified melanoma cells in the volar skin has not been studied. We thus tested the distribution of *CCND1*-amplified cells in the lesional skin by DNA-FISH analysis. As shown in Figure 6A, *CCND1*-amplified cells were found in the SP in multiple cases of early acral melanoma, which were originally evaluated as melanoma *in situ* (n = 3/4 cases) with their contiguous distribution along the duct up to the epidermis. It is

notable that the *CCND1* amplification level in melanoma cells is significantly higher in the epidermis than in the SP (Figure 6B and data not shown). The opposite pattern (less amplification in the epidermis) has not been found in any acral melanoma cases examined. The significant increase in *CCND1* gene amplification level in the epidermis indicates that melanoma cells in the SP not only maintain themselves in an immature unpigmented state in particular gland(s) but also can provide their amplifying progeny, which then undergo more amplification in the epidermis. We thus concluded that the SP of acral sweat glands serves as the reservoir of early melanoma precursors which can generate noticeably mature melanoma cells with more oncogenic alterations and expansion in the epidermis (Figure 6C).

Discussion

In this study, we identified McSCs, which possess somatic stem cell characteristics, in sweat glands in murine volar skin. We found that the SP of the sweat glands are the anatomical niche not only for those melanoblasts but also for early human melanoma precursors with *CCND1* gene amplification. As far as we know, this is the first identification of the niche for oncogenically mutated early cancer cells in human solid cancer tissues, while leukemogenic mutations such as *BCR-ABL* mutations have been found in hematopoietic stem cells (Rossi et al., 2008), the exact niche for early cancer cells remain unknown even in solid cancer as far as we know. Visually detectable pigmentation of the earliest melanoma *in situ* lesions such as those with a few mm in diameter is the suitable system to tackle this problem and allowed us to search for the niche where melanoblasts with early genetic melanoma alteration are hiding deep in the skin.

McSCs in sweat glands are an extremely rare population in the skin compared with McSCs in hair follicles and are more resistant to X-ray, but possess many similar stem cell characteristics. They are normally immature and slow-cycling but transiently renew themselves not only physiologically but also in response to genotoxic stress and provide an amplifying and differentiating progeny into the epidermis through the ascending sweat duct which connect the SP to the epidermis. As those McSCs are maintained in an immature and quiescent state in the SP, where sweat gland keratinocytes are also maintained in a quiescent state (Lu et al., 2012; Nakamura and Tokura, 2009), both in mice and in humans, the SP seem to provide a special niche microenvironment for a fixed number of McSC-like cells in an inactivated immature state (shown schematically in Figure 6C scheme). In contrast, immature but amplifying McSC-like cells or immature melanoma precursor cells in human volar skin were found in the SP of particular sweat glands of early acral melanoma lesions. As these McSC-like cells do not form a tumor mass within the SP, but amplifying and differentiating melanoma cells are distributed in the upper area of the gland(s) and the surrounding epidermis, it is most likely that mutated McSC-like cells in the SP keep providing their amplifying and differentiating progeny toward the epidermis as tumor-initiating cells or cancer stem cells. The melanoma cell distribution pattern, the *CCND1* amplification pattern in the SP versus in the epidermis of those early melanoma cases, and the immaturity of those melanoma cells in the SP collectively suggest that the McSC-like cells in the SP are the initial origin of human acral melanoma at least in some cases. As copy number amplification requires the DNA replication process (Hastings et al., 2009), it is most likely that these mutated McSC-like cells in the SP of particular sweat gland(s) generate more amplified subclones which expand for further progression outside of their niche mainly in the epidermis during early melanomagenesis. The origin of melanoma cells, thus, may explain the preferential proliferation and pigmentation of acral melanoma cells in the CPI around epidermal ducts. However, our data do not exclude the possibility that some acral melanomas also originate directly from epidermal melanocytes and migrate down to the SP of some sweat glands to colonize the niche and become unpigmented and obtain the immature property common to McSCs upon their colonization of the SP (Figure 6C and Figure S14). Recently reported melanoma variant called 'syringotropic melanoma', which shows the prominent involvement of sweat glands (Zembowicz and Kafanas, 2012) may represent one of the two possibilities. The radial distribution pattern of melanoma cells from the sweat glands suggests that melanoma cells can be originated from McSC-like cells in the SP of sweat glands, but further studies are necessary. In either case, our data indicated that sweat glands provide an anatomical niche not only for normal McSC-like cells but also for early melanoma cells in the volar skin and suggested that renewing melanoma cells with early genetic alteration (s) in the SP can further evolve into subclones with more genetic alterations within the epidermis.

Moreover, the fact that acral McSC-like cells are activated to renew themselves upon genomic stress such as IR may explain the IR-refractory characteristics and genomic instability frequently found in early acral melanoma (Curtin et al., 2005). As amplifying McSC-like cells or melanoma precursors with an oncogenic mutation reside in the SP located deep in the subcutaneous fat, sufficient deep surgical excision of the niche lesion and accurate staging of acral melanoma with careful evaluation of tumor depth and involvement of McSC-like melanoma precursors may improve the prognosis of melanoma patients. Further studies on the melanocyte precursors as a melanoma origin or tumor-initiating cells, their topographical dynamics for clonal evolution, and their potential for therapeutic target are necessary to combat this devastating cancer.

Methods

See Supporting Information for detailed methods.

Mice

Dct-H2B-GFP mice were newly generated as described in Supporting Information. *Dct-LacZ* transgenic mice were a kind gift from Dr. Ian Jackson. *Mitf-ce* mice were a kind gift from Dr. M. Lynn Lamoreux (Zimring et al., 1996).

BrdU injection

Mice were injected subcutaneously at 24-h intervals with 20 μl BrdU solution in PBS at 2 mg/ml.

ACK2 treatment

For the treatment of neonatal mice, 200 μg ACK2 was injected into the peritoneal cavity at days 0, 2, and 4 after birth (Nishimura et al., 2002). For the treatment of adult mice, 1 mg ACK2 was injected into the peritoneal cavity at the days 1, 3, 5, 7, and 9 after plucking at P49.

Irradiation

Mice were irradiated at a dose of 5 Gy using 1.0-mm aluminum filters as previously described (Inomata et al., 2009).

Histology

Immunohistochemistry was performed as previously described (Inomata et al., 2009).

Acknowledgements

We thank Dr. Ian Jackson (Roslin Institute) for the *Dct-LacZ* mice; Dr. Vincent Hearing (National Cancer Institute) for antibodies; Dr. David Fisher (Harvard Medical School) for antibodies; Dr. Shinichi Nishikawa (RIKEN C.D.B.) for plasmid; Dr. Ryuhei Okuyama (Shinsyu University) for his support; Dr. Robert Hoffman (University of California, San Diego) for his critical reading of the manuscript; Dr. Hatsune Makino (National Research Institute for Child Health and Development) for her support for human samples; Dr. Ken Inomata for his support for experiments; and Dr. Hideaki Tanizaki and Dr. Yo Kaku for skin excision surgery at Kyoto University. E.K.N is supported by JSPS Funding Program for Next Generation World-leading Researchers (NEXT Program) and Grant-in-Aid for Scientific Research on Innovative Areas.

Conflict of interests

The authors declare no competing financial interests.

References

Cable, J., Jackson, I.J., and Steel, K.P. (1995). Mutations at the W locus affect survival of neural crest-derived melanocytes in the mouse. Mech. Dev. *50*, 139–150.

Cotsarelis, G., Sun, T.-T., and Lavker, R.M. (1990). Label-retaining cells reside in the bulge area of pilosebaceous unit: implications for follicular stem cells, hair cycle, and skin carcinogenesis. Cell *61*, 1329–1337.

Curtin, J.A., Fridlyand, J., Kageshita, T. et al. (2005). Distinct sets of genetic alterations in melanoma. N. Engl. J. Med. *353*, 2135–2147.

Fuchs, E., Tumbar, T., and Guasch, G. (2004). Socializing with the neighbors: stem cells and their niche. Cell *116*, 769–778.

Ganss, R., Montoliu, L., Monaghan, A.P., and Schutz, G. (1994). A cell-specific enhancer far upstream of the mouse tyrosinase gene confers high level and copy number-related expression in transgenic mice. EMBO J. *13*, 3083–3093.

Garbe, C., Eigentler, T.K., Keilholz, U., Hauschild, A., and Kirkwood, J.M. (2011). Systematic review of medical treatment in melanoma: current status and future prospects. Oncologist *16*, 5–24.

Hastings, P.J., Lupski, J.R., Rosenberg, S.M., and Ira, G. (2009). Mechanisms of change in gene copy number. Nat. Rev. Genet. *10*, 551–564.

Inomata, K., Aoto, T., Binh, N.T. et al. (2009). Genotoxic stress abrogates renewal of melanocyte stem cells by triggering their differentiation. Cell *137*, 1088–1099.

Kanda, T., Sullivan, K.F., and Wahl, G.M. (1998). Histone-GFP fusion protein enables sensitive analysis of chromosome dynamics in living mammalian cells. Curr. Biol. *8*, 377–385.

Kingsbury, S.R., Loddo, M., Fanshawe, T., Obermann, E.C., Prevost, A.T., Stoeber, K., and Williams, G.H. (2005). Repression of DNA replication licensing in quiescence is independent of geminin and may define the cell cycle state of progenitor cells. Exp. Cell Res. *309*, 56–67.

Larue, L., and Beermann, F. (2007). Cutaneous melanoma in genetically modified animals. Pigment Cell Res. *20*, 485–497.

Li, L., and Clevers, H. (2010). Coexistence of quiescent and active adult stem cells in mammals. Science *327*, 542–545.

Lu, C.P., Polak, L., Rocha, A.S., Pasolli, H.A., Chen, S.-C., Sharma, N., Blanpain, C., and Fuchs, E. (2012). Identification of stem cell populations in sweat glands and ducts reveals roles in homeostasis and wound repair. Cell *150*, 136–150.

Mackenzie, M.A.F., Jordan, S.A., Budd, P.S., and Jackson, I.J. (1997). Activation of the receptor tyrosine kinase kit is required for the proliferation of melanoblasts in the mouse embryo. Dev. Biol. *192*, 99–107.

Makino, T., Yanagihara, M., Oiso, N., Mizawa, M., and Shimizu, T. (2013). Repigmentation of the epidermis around the acrosyringium in piebald skin: an ultrastructural examination. Br. J. Dermatol. *168*, 910–912.

Mocellin, S., Pasquali, S., Rossi, C.R., and Nitti, D. (2010). Interferon alpha adjuvant therapy in patients with high-risk melanoma: a systematic review and meta-analysis. J. Natl Cancer Inst. *102*, 493–501.

Nakamura, M., and Tokura, Y. (2009). The localization of label-retaining cells in eccrine glands. J. Invest. Dermatol. *129*, 2077–2078.

Nijnik, A., Woodbine, L., Marchetti, C. et al. (2007). DNA repair is limiting for haematopoietic stem cells during ageing. Nature *447*, 686–690.

Nishimura, E.K. (2011). Melanocyte stem cells: a melanocyte reservoir in hair follicles for hair and skin pigmentation. Pigment Cell Melanoma Res. *24*, 401–410.

Nishimura, E.K., Jordan, S.A., Oshima, H., Yoshida, H., Osawa, M., Moriyama, M., Jackson, I.J., Barrandon, Y., Miyachi, Y., and Nishikawa, S.-I. (2002). Dominant role of the niche in melanocyte stem-cell fate determination. Nature *416*, 854–860.

Nishimura, E.K., Granter, S.R., and Fisher, D.E. (2005). Mechanisms of hair graying: incomplete melanocyte stem cell maintenance in the niche. Science *307*, 720–724.

Nishimura, E.K., Suzuki, M., Igras, V., Du, J., Lonning, S., Miyachi, Y., Roes, J., Beermann, F., and Fisher, D.E. (2010). Key roles for transforming growth factor-beta in melanocyte stem cell maintenance. Cell Stem Cell *6*, 130–140.

North, J.P., Kageshita, T., Pinkel, D., Leboit, P.E., and Bastian, B.C. (2008). Distribution and significance of occult intraepidermal tumor cells surrounding primary melanoma. J. Invest. Dermatol. *128*, 2024–2030.

Oguchi, S., Saida, T., Koganehira, Y., Ohkubo, S., Ishihara, Y., and Kawachi, S. (1998). Characteristic epiluminescent microscopic

